Journal of Chromatography, 544 (1991) 147–184
Elsevier Science Publishers B.V., Amsterdam

CHROM. 22 941

Review

Hydroxyapatite as a liquid chromatographic packing

TSUTOMU KAWASAKI
Chromatographic Research Laboratory, Koken Bioscience Institute, 3–5–18 Shimo-Ochiai, Shinjuku-Ku, Tokyo 161 (Japan)

ABSTRACT

A general review of both classical and recent research on hydroxyapatite chromatography is presented, with the main purpose of establishing the specific mechanism involved in this type of chromatography. The deductions were confirmed with the aid of a crystallographic study of hydroxyapatite, adsorption experiments and quantitative analysis on the basis of a general theory of gradient chromatography. The mutual separation of proteins and other biomacromolecules with subtle structural differences is highly specific to hydroxyapatite chromatography.

CONTENTS

0021-9673/91/$03.50

1. INTRODUCTION

Hydroxyapatite [HA; $Ca_{10}(PO_4)_6(OH)_2$] column chromatography, a powerful technique for the separation of proteins, nucleic acids and viruses in aqueous systems, is often carried out by using a linear molarity gradient of potassium or sodium phosphate buffer at pH $\approx$ 6.8 [*i.e.*, an equimolar mixture of K_2HPO_4 and KH_2PO_4 (KP buffer) or an equimolar mixture of Na_2HPO_4 and NaH_2PO_4 (NaP buffer)]. In addition to this standard method, there are a variety of directions for use (see sections 2, 3 and 6). In general, the chromatography should be carried out at pH values higher than about 5, where the crystal structure of HA is thermodynamically stable.

HA chromatography was originally introduced in 1956 by Tiselius *et al.* [1]. From 1959 to the early 1970s, a number of experiments were carried out by Bernardi's group with the purpose of elucidating the fundamental chromatographic mechanism. This was reviewed by Bernardi [2–4]. In 1972, HA chromatography in the presence of a detergent was reported by Moss and Rosenblum [5]. In 1973–74, the interaction mechanism between nucleic acid and HA was explored by Martinson and Wagenaar *e.g.*, [6,7]). In 1978, the chromatographic properties of several types of HA prepared by using different methods were studied by Spencer [8,9] in connection with both the crystal surface structure (as observed by scanning electron microscopy) and the size of the crystallites constituting the total HA particle (as deduced from the X-ray diffraction profile). In 1984, the experimental investigations initiated in Bernardi's laboratory were continued by Gorbunoff and Timasheff [10–12]. In all the above experiments, open columns were used.

In 1983, stainless-steel columns for high-performance liquid chromatography (HPLC) packed with Tiselius-type HA [1] were first made commercially available by Bio-Rad Labs. (Richmond, CA, U.S.A.), followed by Koken (Tokyo, Japan), accompanied by two scientific papers [13,14]. (Tiselius-type HA as presented in refs. 13 and 14 will henceforth be called HA type H.) Slightly retarded HPLC columns packed with coral HA (constructed by aggregation of hexagonal rods) were introduced by Mitsui Toatsu Chemicals (Tokyo, Japan). The first paper on the use of an HPLC column packed with spherical HA with an average diameter of *ca.* 5 μm [constructed by aggregation of microcrystals; called HA type S (Fig. 1)] was published in 1986 by Kawasaki *et al.* [15], followed by a second paper [16]. Almost at the same time, an independent study with a spherical HA packed HPLC column was published by Kadoya *et al.* [17]. In parallel with the appearance of these papers [15–17], spherical HA packed columns were made commercially available by Koken, Tonen and Asahi Optical (all Tokyo, Japan). The first company treated the HA particles described in refs. 15 and 16 by adding particles with an average diameter of *ca.* 20 μm; HPLC columns packed with these particles are also available from Regis Chemical (Morton Grove, IL, U.S.A.). The last two companies used HA particles as described in ref. 17. About 1 year later, two other types of spherical HA packed columns were introduced by Tosoh (Tokyo, Japan), followed by Cica-Merck (Tokyo, Japan); the first column was accompanied by the publication of a scientific paper [18]. HPLC columns packed with square tile-shaped HA (called HA type F) were also made available by Koken, accompanied by a scientific paper [19]. (Scanning electron micrographs of the surface structures of HA type H, coral HA, HA type S and HA type F are presented later in Fig. 9.)

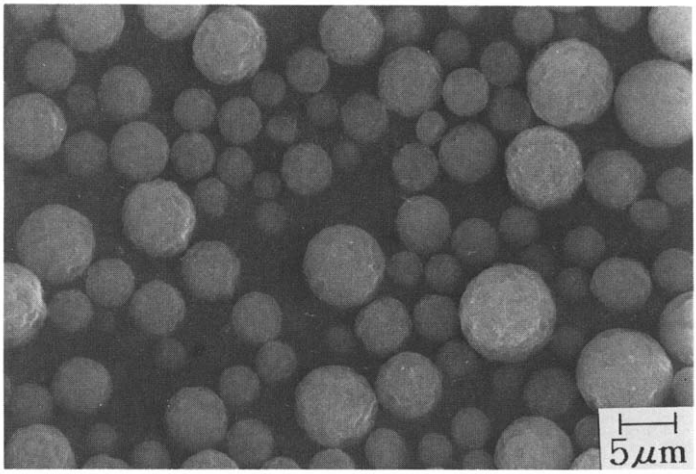

Fig. 1. Scanning electron micrograph of spherical HA type S with an average diameter of *ca.* 5 μm. The surface structure of the particle is shown in Fig. 9b. (Photograph by courtesy of Dr. H. Monma, National Institute for Research in Inorganic Materials, Tsukuba, Japan.)

An HPLC column packed with spherical particles of strontium phosphate $HA[Sr_{10}(PO_4)_6(OH)_2]$ was developed by Kawasaki *et al.* [20] and an HPLC column packed with spherical particles of fluoroapatite $[Ca_{10}(PO_4)_6F_2]$ by Sato *et al.*[21].

A method of separating acidic and basic proteins from each other by applying double gradients of KCl (or NaCl) and KP (or NaP) buffer was introduced by Kawasaki *et al.* [14] (see section 3). A novel technique of chromatographing uncharged glycoside molecules on an HA column in the presence of a high concentration (*e.g.*, 70–90%) of acetonitrile was introduced by Kasai *et al.* [22] (see section 6).

HA-type HPLC columns have been applied with success for the mutual separation of different molecular species of proteins such as protein kinase C [23], heat-shock protein [24] and human tumour necrosis factor protein (see section 5) and different molecular species of t-RNA [25]. This type of column has also been applied to the purification of cytochrome P-450 [26], bradykinin-hydrolysing enzyme [27], etc.

2. LOOKING BACK ON CLASSICAL WORK CARRIED OUT BY USING OPEN COLUMNS PACKED WITH TISELIUS-TYPE HYDROXYAPATITE: FUNDAMENTAL CHROMATOGRAPHIC MECHANISMS DEDUCED FROM THESE DATA

The purpose of this section is to review important aspects of experimental investigations on HA chromatography with aqueous systems that were carried out mainly by Bernardi [2–4] and Gorbunoff and Timasheff [10–12], from which chromatographic mechanisms can be deduced. Although the deductions made in this section partially overlap with those made elsewhere [2–4,10–12], several modifications are added on the basis of our own opinions; the deductions made in refs. 10–12 are partially very different from ours (see below).

With regard to the chromatography of nucleic acids and other nucleotides, the experiments below are of particular importance when considering the chromato-

graphic mechanism. Thus, by using a linear molarity gradient of KP, native DNAs ranging in molecular mass from 10^5 to 10^7 dalton are usually eluted in the phosphate molarity range 0.20–0.25 *M* [2]. If chromatography is carried out under conditions of constant ionic strength by using 1 m*M* KP–1 *M* KCl as the initial buffer and 0.5 *M* KP as the final buffer, the DNA is eluted at the same phosphate molarity as in the absence of KCl [2]; the KP (or the NaP) molarity means the phosphate molarity in the KP (or the NaP) buffer. This demonstrates that the elution of DNA is not induced by a simple increase in ionic strength. It can be deduced that the elution is caused by phosphate ions from the buffer, and that neither potassium nor chloride ions participate in the chromatographic mechanism. This deduction is supported by the fact that DNA cannot be eluted from the column by either 3 *M* KCl or 3 *M* $CaCl_2$ [28].

As far as the behaviours of nucleotides, some coenzymes and their mono- and polyphosphate derivatives are concerned, non-phosphorylated materials are not retained by the column equilibrated with 1 m*M* KP [2]. The elution of nucleoside monophosphates is slightly retarded in the presence of 1 m*M* KP, and nucleoside di-, tri- and tetraphosphates are eluted at increasingly higher characteristic KP molarities (for details, see ref. 2). This indicates that the molecular retention is caused by phosphate group(s).

It can now be deduced that the mechanism of HA chromatography resembles that of anion-exchange chromatography: competition occurs between nucleic acids (with adsorption of phosphate groups) and phosphate ions from the buffer for adsorption on crystal surfaces of the HA particles packed in the column. The nucleic acid molecules initially adsorbed at the inlet of the column, forming a narrow band, are driven out of the crystal surface by competing phosphate ions. Chloride ions, although they are anions, are not adsorbed on the HA surface, presumably owing to a steric hindrance.

With regard to chromatography of synthetic polypeptides, those which have no carboxyl or basic (*e.g.*, ε-amino, δ-amino or guanidinyl) groups, except for a minor proportion of the terminal groups (poly-L-Tyr, poly-L-Ser, poly-L-Pro, poly-D,L-His, and copoly-L-benzyl-Glu-D,L-His) are not retained on the column, and those which have either carboxyl or basic groups (poly-L-Asp, poly-L-Glu, poly-L-Lys, poly-L-Orn, poly-L-Arg, copoly-L-Glu-L-Lys, copoly-L-Glu-L-Phe and copoly-L-Glu-L-Ser) are retained [3,4]. From these results, it can be deduced that charged groups are generally responsible for the adsorption of polypeptides on the HA surface.

Polypeptides that have carboxyl groups and no basic groups, *e.g.*, poly-L-Asp and poly-L-Glu, are eluted by a linear KP molarity gradient at about 0.35 and 0.25 *M*, respectively [3]. Carrying out the elution at constant ionic strength by using 1 m*M* KP–1 *M* KCl as the initial buffer and 0.5 *M* KP as the final buffer does not change the phosphate molarity for elution of poly-L-Glu [3], which cannot be eluted from the column by either 3 *M* KCl or 3 *M* $CaCl_2$ [28]. It can be deduced from these data that the elution mechanism of acidic polypeptides is similar to that of nucleic acids: competition occurs between acidic polypeptides (with adsorption of carboxyl groups) and phosphate ions from the buffer for adsorption on the HA surface. Statistical copolymers of poly-L-Glu involving minor proportions of Phe, Ser and Lys are eluted at slightly lower molarities of the KP gradient than poly-L-Glu [3,29]; this also implies that carboxyl groups are responsible for the adsorption of acidic polypeptides.

Polypeptides that have basic groups and no carboxyl groups (poly-L-Lys,

poly-L-Orn, and poly-L-Arg) cannot be eluted from the column even by using a KP molarity gradient reaching a phosphate molarity of 1 *M* [3,4]. With a low-molecular-mass poly-L-Lys, however, a large aliquot of the retained material is eluted with a 1 m*M*–1 *M* NaP gradient as a series of sharp peaks [3,4][a]. In contrast to acidic polypeptides, basic polypeptides can be eluted from the column by 3 *M* NaCl, 3 *M* KCl or a low molarity of $CaCl_2$ [3,4,28].

With regard to the chromatography of native proteins, important data taken from refs. 4, 10–12 and 28 are summarized in Table 1, which shows the elution molarities of 26 proteins with different isoelectric points (p*I*) obtained by applying linear molarity gradients of KP, KCl, NaP, NaCl, NaF, $CaCl_2$ and $MgCl_2$. Table 1 shows that the chromatographic behaviour of acidic molecules (with p$I \lesssim 7$) is completely different from that of basic molecules (with p$I \gtrsim 7$) in most instances. For example, it can be seen in Table 1 that the elution molarities of only acidic proteins are generally much enhanced in both KCl and NaCl systems (the 6th and 10th columns) in comparison with the elution molarities in both KP and NaP systems (the 4th, 5th, 8th and 9th columns); both of the ratios $m_{elu(KCl)}/m_{elu(K^+;KP)}$ (7th column) and $m_{elu(NaCl)}/m_{elu(Na^+;NaP)}$ (the 11th column) are generally much larger than unity with molecules with p$I \leqslant 7.6$ (*i.e.*, proteins 1–17), except for protein 11 (with a ratio of 0.59) and protein 12 (with a ratio of 0.72). For molecules with p$I \geqslant 8.1$ (*i.e.*, proteins 18–26), however, the ratio under consideration is always of the order of unity. (It should be noted that there are only slight differences in elution molarities between the KP and the NaP system; *cf.*, elution molarities for proteins 8, 16, 18, 22, 23 and 26.)

The difference in chromatographic behaviour between acidic and basic proteins is still emphasized in both $CaCl_2$ and $MgCl_2$ systems in which divalent cations are present (see the 14th and 15th columns in Table 1). Thus, with the $CaCl_2$ system, the elution molarities for the proteins with p$I \leqslant 7.6$ and a protein with p$I = 9.3$ (*i.e.*, proteins 1–17, 20) exceed 3.0 *M* whereas the proteins with p$I \geqslant 8.1$, except for a protein with p$I = 9.3$ (*i.e.*, proteins 18, 19, 21–26), are eluted at extremely low molarities between 1 and 10 m*M* (see the 14th column in Table 1). With the $MgCl_2$ system also a similar result is obtained, except that the elution molarities of some proteins (proteins 3, 6, 11 and 20) decrease considerably in comparison with the $CaCl_2$ system (see the 15th column in Table 1).

The fact that the elution molarities of acidic proteins are generally much enhanced in the KCl, NaCl, $CaCl_2$ and $MgCl_2$ systems is parallel with the results for both nucleic acids and acidic polypeptides (see above). This implies that the chromatographic mechanism for acidic proteins also resembles that of anion-exchange chromatography.

It can be seen in Table 1 that the elution molarities in the NaF system (12th column) are parallel with those in the NaP system (8th and 9th columns). As a result, the ratio $m_{elu(NaCl)}/m_{elu(NaF)}$ is much larger than unity with proteins with p$I \leqslant 7.6$, except for a protein with p$I = 5.3$, whereas the proteins with p$I \geqslant 8.1$ and the protein with p$I = 5.3$ have a ratio of the order of unity (see the 13th column in Table 1). These data imply that, in contrast to chloride ions and similarly phosphate ions, fluoride ions

[a] In refs. 3 and 4, it is mentioned that the KP gradient was applied instead of the NaP gradient; this is an error (Professor Bernardi, personal communications).

can be adsorbed on the HA surface and that they compete with acidic proteins for adsorption.

Among the univalent cation systems (*i.e.*, KP, KCl, NaP, NaCl and NaF systems), the potassium or sodium molarities for elution are of the same order of magnitude for any given basic protein with p$I \geqslant 8.1$ (see the 5th, 6th, 9th, 10th and 12th columns in Table 1). Among the divalent cation systems (*i.e.*, both $CaCl_2$ and $MgCl_2$ systems) also the elution molarities are of the same order of magnitude for any

TABLE I

ELUTION MOLARITIES OF 26 PROTEINS WITH DIFFERENT ISOELECTRIC POINTS OBTAINED BY APPLYING MOLARITY GRADIENTS OF SEVERAL INORGANIC SALTS

The data for the KP and KCl systems and the data for the NaP, NaCl, NaF and $MgCl_2$ systems have been taken from refs. 4 and 28 and refs. 10–12, respectively. As far as the $CaCl_2$ system is concerned, the data for proteins 1, 9, 14 and 24 have been taken from refs. 4 and 28, those for proteins 8, 16, 18, 22, 23 and 26 from both refs. 4 and 28 and refs. 10–12 and those for the other proteins from refs. 10–12. The elution molarity for protein 16 in the NaP system and that for protein 26 in the KP system represent new values that have been re-determined recently in our laboratory. A column of 18–23 cm × 1 cm I.D. was used with both KP and KCl systems and also the $CaCl_2$ system for proteins 1, 9, 14 and 24; the data for proteins 8, 16, 18, 22, 23 and 26 were partially obtained by using this column [4,28]. A column of 20 cm × 1 cm I.D. was used with the other systems; the data for proteins 8, 16, 18, 22, 23 and 26 partially were obtained by using this column [10–12]. With the KP system, the elution was carried out by using a linear KP gradient with both $g'_{(P)} = 2.4$ mM/ml [$g'_{(K^+)} = 3.6$ mM/ml] and $m_{in(P)} = 10$ mM [4,28]. With the KCl system, the elution was carried out in the presence of 10 mM KP by using a linear KCl gradient with both $g'_{(KCl)} = 5$–7.5 mM/ml and $m_{in(KCl)} = 0$ M [4,28]. With the NaP system, the elution was carried out by using a linear NaP gradient with both $g'_{(P)} \approx 2.5$ mM/ml [$g'_{(Na^+)} \approx 3.75$ mM/ml] and $m_{in(P)} = 10$ mM [10]. With the NaCl and the NaF systems, the elution was carried out in the presence of 10 mM NaP by using a linear NaCl and a linear NaF gradient, respectively, where $g'_{(NaCl)} = g'_{(NaF)} \approx 2.5$ mM/ml and $m_{in(NaCl)} = m_{in(NaF)} = 0$ M [10]. With the $CaCl_2$ system, the step elution method was applied in part (for details, see refs. 4, 10 and 28). As far as the $MgCl_2$ system is concerned, the experimental conditions have not been described in the literature [10–12]. It can tacitly be understood, however, that the experiment was performed under conditions similar to those for the $CaCl_2$ system [12].

No.	Protein	pI	KP system		KCl system, $m_{elu(KCl)}$	$\frac{m_{elu(KCl)}}{m_{elu(K^+;KP)}}$
			$m_{elu(P)}$	$m_{elu(K^+)}$		
1	Pepsin	1.0	0.03	0.045	>3.0	>67
2	Lima bean trypsin inhibitor	3.5–5.0				
3	Ovamucoid	3.8–4.5				
4	Pepsinogen	3.9				
5	Soybean trypsin inhibitor	4.5				
6	α-Lactalbumin	4.5				
7	Ovalbumin	4.6				
8	Bovine serum albumin	4.7	0.06	0.09	>3.0	>33
9	Pancreatic deoxyribonuclease	4.7	0.04	0.06	0.40	6.7
10	β-Lactoglobulin A	5.1–5.3				
11	Carbonic anhydrase B	5.3				
12	Catalase (bovine liver)	5.4				
13	Insulin	5.5				
14	Snail acid deoxyribonuclease	5.9	0.11	0.165	0.54	3.3
15	Conalbumin	6.8				
16	Myoglobin	7.0	0.12	0.18	0.80	4.4
17	Haemoglobin (horse)	7.6				
18	α-Chymotrypsin	8.1–8.6	0.16	0.24	0.32	1.3
19	γ-Chymotrypsin	8.5				
20	Trypsinogen	9.3				
21	Chymotrypsinogen	9.5				
22	Ribonuclease A	9.7	0.12	0.18	0.23	1.3
23	Cytochrome *c*	9.8–10.6	0.23	0.345	0.48	1.4
24	Spleen acid deoxyribonuclease	10.2	0.22	0.33	0.44	1.4
25	Papaya lysozyme	10.5				
26	Lysozyme (chicken)	10.5–11.0	0.19	0.285	0.25	0.87

given basic protein with p$I \geqslant 8.1$, except for a protein with p$I = 9.3$ (protein 20), and the elution molarities for the basic proteins in the divalent cation systems (except for protein 20) are generally much lower than those in the univalent cation system (see the 14th and 15th columns in Table 1). These data lead to the deduction that the chromatographic mechanism for basic proteins resembles that of cation-exchange chromatography: competition occurs between basic proteins (with adsorption of ε-amino and guanidinyl groups) and cations (K^+, Na^+, Ca^{2+} and Mg^{2+} ions) for

Symbols:
$m_{elu(P)}$ = elution molarity concerning phosphate ions with the KP or NaP gradient.
$m_{elu(K^+)}$ or $m_{elu(K^+;KP)}$ = elution molarity concerning potassium ions with the KP gradient.
$m_{elu(Na^+)}$ or $m_{elu(Na^+;NaP)}$ = elution molarity concerning sodium ions with the NaP gradient.
$m_{elu(KCl)}$ = elution molarity with the KCl gradient; this is equal to the elution molarity concerning potassium ions.
$m_{elu(NaCl)}$ = elution molarity with the NaCl gradient; this is equal to the elution molarity concerning sodium ions.
$m_{elu(NaF)}$ = elution molarity with the NaF gradient; this is equal to the elution molarity concerning either sodium or fluoride ions.
$m_{elu(CaCl_2)}$ = elution molarity with the $CaCl_2$ gradient; this is equal to the elution molarity concerning calcium ions.
$m_{elu(MgCl_2)}$ = elution molarity with the $MgCl_2$ gradient; this is equal to the elution molarity concerning magnesium ions.
$m_{in(X)}$ = initial molarity concerning substance X, occurring before the gradient begins. X may be P (*i.e.*, phosphate ion), K^+, Na^+, KCl, NaCl, NaF, $CaCl_2$ or $MgCl_2$.
$g'_{(X)}$ = slope of the molarity gradient concerning substance X, measured in units of M/ml or mM/ml. For substance X, see the explanation for $m_{in(X)}$.
$g'_{(X)}$ (ϕ = 1 cm) = reduced $g'_{(X)}$ to column I.D. ϕ = 1 cm; this symbol will be used later.

NaP system		NaCl system,		NaF system,		$CaCl_2$ system,	$MgCl_2$ system,
$m_{elu(P)}$	$m_{elu(Na^+)}$	$m_{elu(NaCl)}$	$\frac{m_{elu(NaCl)}}{m_{elu(Na^+;NaP)}}$	$m_{elu(NaF)}$	$\frac{m_{elu(NaCl)}}{m_{elu(NaF)}}$	$m_{elu(CaCl_2)}$	$m_{elu(MgCl_2)}$
						>3.0	
0.12	0.18	>3.0	>17	0.12	>25	>3.0	
0.001	0.0015	>3.0	>2000			>3.0	0.1
0.13	0.195	>3.0	>15	0.15	>20	>3.0	>3.0
0.13	0.195	>3.0	>15	0.13	>23	>3.0	>3.0
0.13	0.195	1.8	9.0	0.14	13	>3.0	0.3
0.09	0.135	>3.0	>21	0.12	>25	>3.0	>3.0
0.06	0.09	>3.0	>33	0.13	>23	>3.0	>3.0
						>3.0	
0.24	0.36	>3.0	>8.3	0.66	>4.5	>3.0	
0.11	0.165	0.10	0.59	0.12	0.83	>3.0	0.1
0.12	0.18	0.13	0.72			>3.0	>3.0
0.11	0.165	>3.0	>18	0.15	>20	>3.0	1.0
						>3.0	
0.18	0.27	>3.0	>11	0.13	>23	>3.0	1.0
0.13	0.195	0.60	3.1	0.14	4.3	>3.0	1.0
0.19	0.285	0.66	2.3	0.10	6.6	>3.0	1.0
0.18	0.27	0.26	0.96	0.24	1.1	0.003–0.01	0.003
0.21	0.315	0.30	0.94	0.24	1.25	0.003	
0.17	0.255	0.32	1.3	0.23	1.4	>3.0	0.1
0.19	0.285	0.23	0.81	0.24	0.96	0.002	0.002
0.12	0.18	0.13	0.72	0.13	1.0	0.001	
0.25	0.375	0.32	0.85	0.35	0.91	0.002–0.007	0.003
						0.002	
0.25	0.375	0.25	0.67	0.20	1.3	0.001	
0.18	0.27	0.18	0.67	0.19	0.95	0.001	0.001

adsorption on the HA surface. Divalent cations that can be strongly adsorbed on the HA surface drive basic proteins out of the surface at much lower molarities than univalent cations that can be adsorbed only weakly. The behaviour of basic proteins is consistent with the behaviour of basic polypeptides which can be eluted from the column by 3 *M* NaCl, 3 *M* KCl or a low molarity of $CaCl_2$ (see above).

It is reasonable, in general, to assume that adsorbing sites are arranged on the crystal surface of HA with a minimum inter-site distance of the order of magnitude of the size of a unit crystal cell, or several to ten ångstroms (for details, see section 4.1). On the other hand, inorganic ions participating in chromatography, K^+, Na^+, Ca^{2+}, Mg^{2+}, $H_2PO_4^-$, HPO_4^{2-} and F^- ions, have diameters of 2.6, 1.9, 2.0, 1.3, *ca.* 5, *ca.* 5 and 2.6 Å, respectively, whereas the size of globular proteins with a molecular mass of the order of 10 000–100 000 dalton (such as those appearing in Table 1) is usually in the range from 30 to more than 100 Å. This leads to the deduction that a competing ion, in general, occupies a single crystal site when it is adsorbed (except in some instances) whereas a protein molecule covers more than one site. The fact that the elution of acidic proteins is generally induced by anions except chloride (with a diameter of 3.6 Å) and that the elution of acidic proteins is not induced, or induced only at high molarities, by cations which bring about the elution of basic proteins (see above) leads to the deduction that the domain on the HA surface on which the adsorption of both acidic molecules and anions occurs is different from that on which the adsorption of both basic molecules and cations occurs.

From the chemical structure of $HA[Ca_{10}(PO_4)_6(OH)_2)]$, it can be visualized that one of the two types of adsorbing site (which exists on one of the two active surfaces of HA, playing the role of an anion exchanger; called the C site) is positively charged, and that it is constructed from a single or several crystal calcium ion(s). The other adsorbing site (which exists on the other active surface of HA, playing the role of a cation exchanger; called the P site) is negatively charged, and is constructed from a single or several crystal phosphate ion(s) (for details, see section 4.1). [The fact that the chromatographic behaviour of some proteins on a fluoroapatite column is parallel to that on the HA column [21] implies that crystal hydroxyl ions (in addition to crystal fluoride ions in the case of fluoroapatite) do not interfere directly in the adsorption mechanism.]

It can be considered that a protein molecule can, in general, be adsorbed on HA in two different ways. In the first, the molecule is adsorbed on C sites (existing on the first type of crystal surface) by using carboxyl groups (and/or phosphate groups in the case of phosphoprotein [3]), and in the second, it is adsorbed on P sites (existing on the second type of crystal surface) by using ε-amino and/or guanidinyl groups. Following a statistical-mechanical law, a canonical or a Boltzmann distribution is realized between the two types of adsorption. In many actual instances, however, the Boltzmann distribution is biased towards one of the two extremes, and acidic molecules that have p*I* lower than about 7 are adsorbed mainly on C sites, whereas basic molecules that have p*I* higher than about 7 are adsorbed mainly on P sites. It can be seen in Table 1 that the ratio $m_{elu(KCl)}/m_{elu(K^+;KP)}$ or $m_{elu(NaCl)}/m_{elu(Na^+;NaP)}$ (see the 7th and 11th column) for acidic molecules is generally much larger than unity, but that it is not always equal to infinity; this would mean that an acidic protein is adsorbed mainly on C sites, but that it is partially adsorbed on P sites also (for related problems, see the second footnote in section 3).

It can be deduced that Ca^{2+} ions have a special ability to strengthen the binding of carboxyl groups to C sites, as all the acidic proteins are retained on the column even in the presence of 3 *M* $CaCl_2$ (see the 14th column in Table 1; for this mechanism, see section 4.1).

It should be added that the elution molarity of both DNA and proteins decreases drastically when the molecule is in the denatured state [2,4,29]. This probably arises from the fact that the charged groups available for interaction with adsorption sites of HA in the rigid, ordered structure drastically decrease in number on the "outer surface" of randomly coiled molecules.

The chromatographic mechanism that has been deduced above is partially very different from that proposed by Gorbunoff and Timasheff [10–12], despite the fact that both deductions are based on common experimental data. The discrepancy mainly arises from the fact that, in refs. 10–12, all the interpretations are based on a tacit hypothesis that sodium ions in the molarity gradient do not interfere at all in the chromatographic mechanism whereas ions such as $H_2PO_4^-$, HPO_4^{2-}, Cl^-, F^-, SCN^-, ClO^-, Ca^{2+} and Mg^{2+} do. No comment on this hypothesis is given in refs. 10–12.

3. DOUBLE GRADIENT HPLC: REINFORCEMENT OF THE CLASSICAL DATA LEADING TO THE FUNDAMENTAL CHROMATOGRAPHIC MECHANISM[a]

Fig. 2 illustrates a double gradient chromatogram of DNA. This was obtained by previously applying the KCl gradient after an isocratic elution with 10 m*M* KP; 10 m*M* KP was present while the KCl gradient continued (left-hand side of Fig. 2). The carrier solvent was again replaced with pure 10 m*M* KP, and the KP gradient was finally applied (right-hand side of Fig. 2). It can be seen in Fig. 2 that the DNA peak

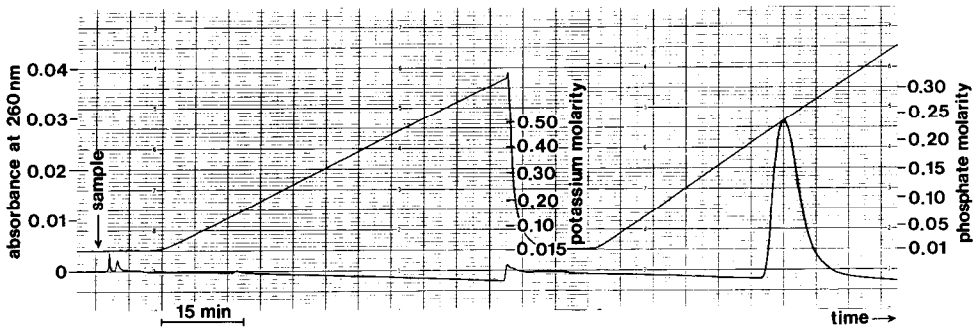

Fig. 2. Double gradient chromatogram of DNA (M.M. = $1 \cdot 10^7$–$1.2 \cdot 10^7$ dalton; from calf thymus), 11 μg, obtained on the HPLC column packed with HA type S (KB column; Koken). Column dimensions: ϕ = 6 mm and L = 3 + 10 = 13 cm. Experimental conditions: $m_{in(P)}$ = 10 m*M* for both KCl and KP gradients; $g'_{(KCl)}$ = 10.4 m*M*/ml [$g'_{(KCl)}$ (ϕ = 1 cm) = 3.75 m*M*/ml]; $g'_{(P;KP)}$ = 6.94 m*M*/ml [$g'_{(P;KP)}$ (ϕ = 1 cm) = 2.5 m*M*/ml]; flow-rate = 1.00 ml/min; P = 2.3–2.8 MPa; T = 25.0°C; recovery = 93%; 10 m*M* KP is always present in the KCl gradient. The gradients were monitored by measuring the refractive index in a special flow cell with a low angle; the same technique will also be used in Figs. 3–7 and 18.

[a] In addition to those given in Table 1, the following symbols are used: M.M. = molecular mass; L = total column length; $L = a + b$ means that the total column of length L is constituted of the precolumn part with length a and the main column part with length b; P = pressure drop; T = temperature.

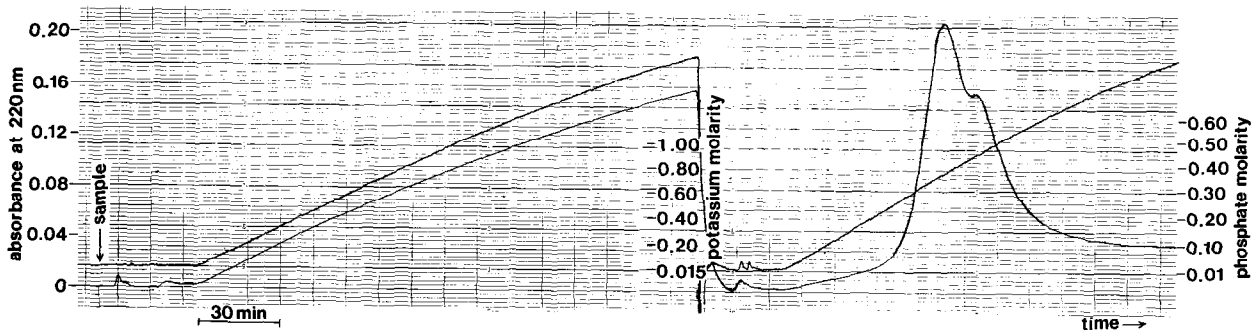

Fig. 3. Double gradient chromatogram of poly-L-Asp (M.M. = 11 500 dalton on average), 0.6 mg, obtained on the KB column with dimensions identical with those in Fig. 2. Experimental conditions: $m_{in(P)}$ = 10 mM for both KCl and KP gradients; $g'_{(KCl)}$ = 20.8 mM/ml [$g'_{(KCl)}$ (ϕ = 1 cm) = 7.5 mM/ml]; $g'_{(P;KP)}$ = 13.9 mM/ml [$g'_{(P;KP)}$ (ϕ = 1 cm) = 5.0 mM/ml]; flow-rate = 0.50 ml/min; P = 2.4–2.6 MPa; T = 23.5°C; recovery >100%; 10 mM KP is always present in the KCl gradient.

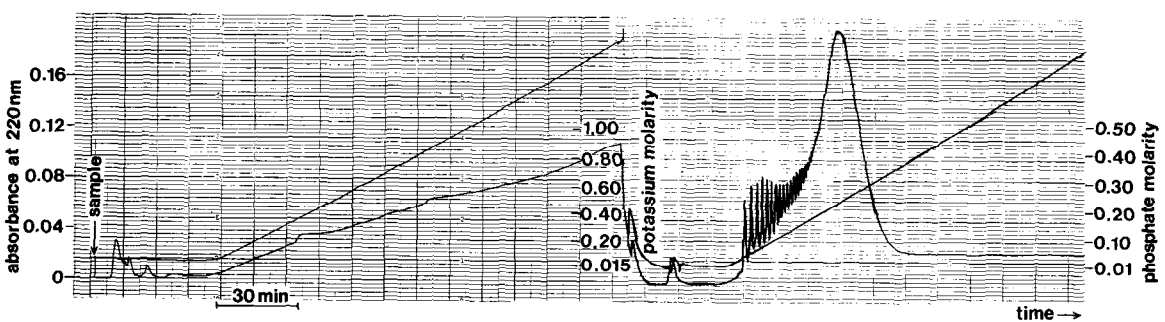

Fig. 4. Double gradient chromatogram of poly-L-Glu (M.M. = 13 600 dalton on average), 1.2 mg, obtained on the KB column with dimensions identical with those in Fig. 2. Experimental conditions: as in Fig. 3, except flow-rate = 0.51 ml/min; P = 2.6–2.9 MPa; T = 23.3°C; recovery = 97%.

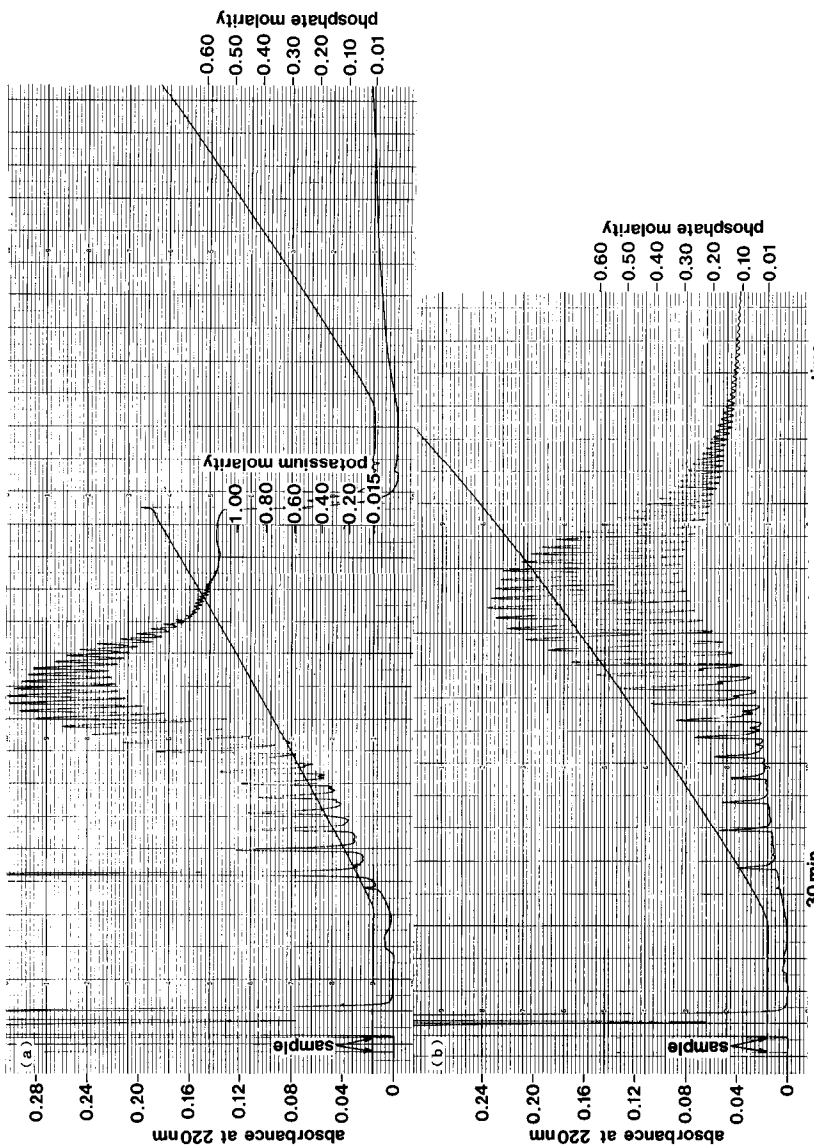

Fig. 5. (a) Double gradient chromatogram of poly-L-Lys (M.M. = 18 000 dalton on average), 4.0 mg, obtained on the KB column with dimensions identical with those in Fig. 2. Experimental conditions: as in Fig. 3, except flow-rate = 0.50 ml/min; P = 2.4–2.6 MPa; T = 24.8°C; recovery >69%. (b) Single KP gradient chromatogram of the same sample (3.0 mg) obtained on the same column. Experimental conditions: $m_{in(P)}$ = 10 mM; $g'_{(P)}$ = 13.9 mM/ml [$g'_{(P)}$ (ϕ = 1 cm) = 5.0 mM/ml]; flow-rate = 0.50 ml/min; P = 2.9–3.1 MPa; T = 25.0°C; recovery >98%.

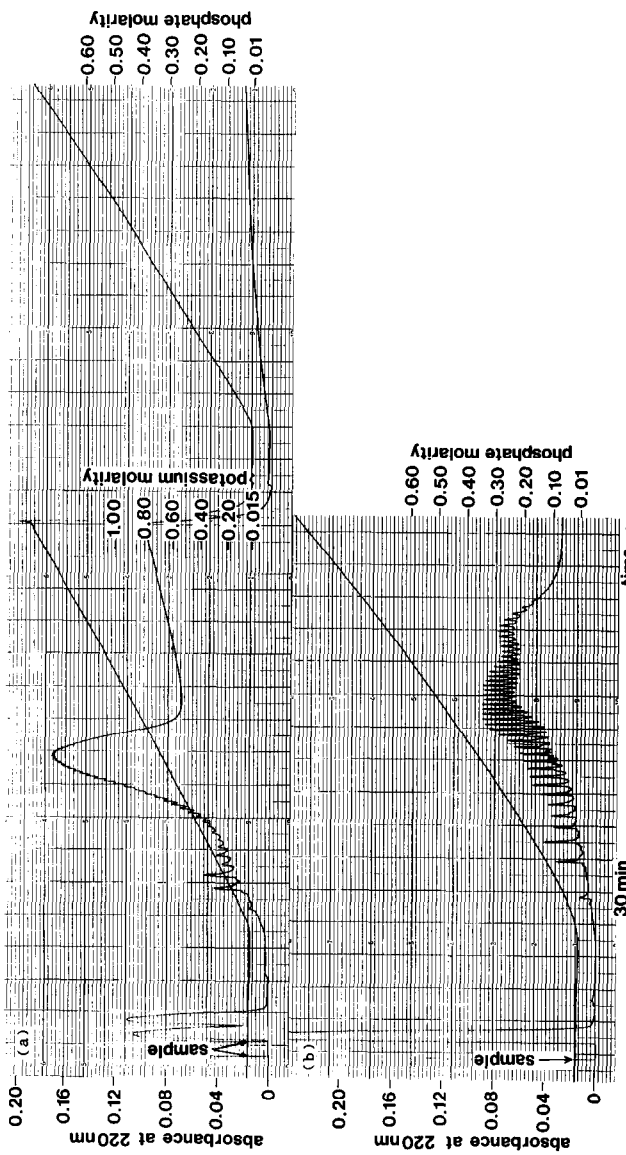

Fig. 6. (a) Double gradient chromatogram of poly-L-Arg (M.M. = 24 000 dalton on average), 2.0 mg, obtained on the KB column with dimensions identical with those in Fig. 2. Experimental conditions: as in Fig. 3, except flow-rate = 0.50 ml/min; P = 2.6–2.9 MPa; T = 27.5°C; recovery = 101%. (b) Single KP gradient chromatogram of the same sample (2.0 mg) obtained on the same column. Experimental conditions: as in Fig. 5b, except flow-rate = 0.50 ml/min; P = 3.3–3.5 MPa; T = 23.0°C; recovery = 100%.

appears in the second KP gradient. It has been confirmed that a DNA chromatogram virtually identical with that obtained in Fig. 2 can be obtained by applying a single KP gradient with a slope, $g'_{(P)}$, equal to that of the KP gradient in the double gradient system.

Figs. 3 and 4 illustrate double gradient chromatograms of poly-L-Asp and poly-L-Glu, respectively; 10 m*M* KP is present while the KCl gradient continues. It can be seen in both Figs. 3 and 4 that these acidic polypeptides are also eluted in the second KP gradient. It has been confirmed that chromatograms virtually identical with those obtained in Figs. 3 and 4 can be obtained by applying a single KP gradient with a slope, $g'_{(P)}$, equal to that of the KP gradient in the double gradient system.

Figs. 5a and 6a illustrate double gradient chromatograms of poly-L-Lys and poly-L-Arg, respectively; 10 m*M* KP is present while the KCl gradient continues. It can be seen in both Figs. 5a and 6a that these basic polypeptides are eluted in the first KCl gradient. Figs. 5b and 6b depict single KP gradient chromatograms that correspond to those in Figs. 5a and 6a, respectively.

By applying a linear $CaCl_2$ gradient with $g'_{(CaCl_2)}$ (ϕ = 1 cm) = 5.0 m*M*/ml (in the absence of phosphate ions) on the KB column with dimensions identical with those for Fig. 2, poly-L-Lys and poly-L-Arg were eluted at molarities lower than 36 m*M* and lower than 10 m*M*, respectively. By applying a linear $MgCl_2$ gradient with $g'_{(MgCl_2)}$ (ϕ = 1 cm) = 5.0 m*M*/ml (also in the absence of phosphate ions), poly-L-Lys

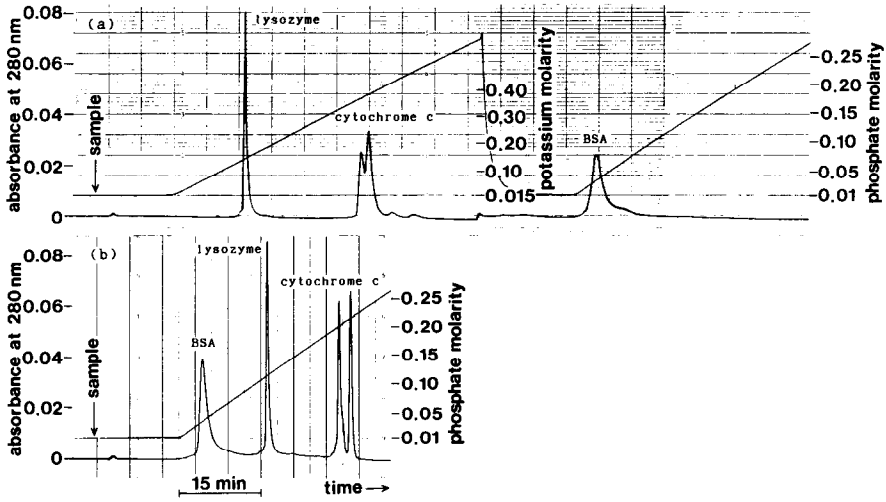

Fig. 7. (a) Double gradient chromatogram for a mixture of BSA (0.17 mg), cytochrome *c* (56 μg) and chicken lysozyme (26 μg) obtained on the KB column with dimensions identical with those in Fig. 2. The first and second peaks in the double peak chromatogram of cytochrome *c* represent the oxidized and the reduced component, respectively [15]. The BSA peak with a large width shows that the molecule is not homogeneous. Experimental conditions: $m_{in(P)}$ = 10 m*M* for both KCl and KP gradients; $g'_{(KCl)}$ = 10.4 m*M*/ml [$g'_{(KCl)}$ (ϕ = 1 cm) = 3.75 m*M*/ml]; $g'_{(P:KP)}$ = 6.94 m*M*/ml [$g'_{(P:KP)}$ (ϕ = 1 cm) = 2.5 m*M*/ml]; flow-rate = 0.97 ml/min; *P* = 1.8–2.1 MPa; *T* = 24.3°C; recovery = 96%. (b) Single KP gradient chromatogram for a mixture of BSA (0.17 mg), cytochrome *c* (56 μg) and chicken lysozyme (26 μg) obtained on the same column. Experimental conditions: $m_{in(P)}$ = 10 m*M*; $g'_{(P)}$ = 6.94 m*M*/ml [$g'_{(P)}$ (ϕ = 1 cm) = 2.5 m*M*/ml]; flow-rate = 0.97 ml/min; *P* = 1.8–2.1 MPa; *T* = 24.3°C; recovery = 107%. (Reproduced from ref. 30.)

was eluted between 14 and 44 mM; poly-L-Arg was eluted at molarities lower than 10 mM. Poly-L-Asp and poly-L-Glu were not eluted at all even in the presence of 3 M $CaCl_2$ or 3 M $MgCl_2$.

Fig. 7a and b illustrate a double gradient chromatogram and a single KP gradient chromatogram, respectively, for a mixture of bovine serum albumin (BSA) (with pI = 4.7), cytochrome c (with pI = 9.8–10.1) and chicken lysozyme (with pI = 10.5–11.0); 10 mM KP is present while the KCl gradient continues. It can be seen in Fig. 7a that BSA with an acidic pI is eluted in the second KP gradient whereas both cytochrome c and lysozyme with basic pI are eluted in the first KCl gradient.

Double gradient experiments were also performed for some nucleoside phosphates and other proteins under experimental conditions similar to those applied in Fig. 7a. It was confirmed that acidic molecules, *i.e.*, ADP, ATP, adenosine tetraphosphate, pepsinogen (pI = 3.7), ovalbumin (pI = 4.6), deoxyribonuclease I (pI = 4.7) and β-lactoglobulin A (pI = 5.1–5.3), are all eluted from the column with the second KP gradient. In some instances with weakly adsorbed proteins, however, a minor proportion of molecules was eluted with a rapid decrease in KCl molarity occurring at the end part of the first KCl gradient. This is presumably due to a kinetic mechanism arising from an abrupt change in the environment (*i.e.*, the KCl molarity); this provokes an abrupt destruction of the stationary state in chromatography. It was confirmed that the molecular elution at the end part of the KCl gradient can be avoided by decreasing the KCl molarity slowly. In contrast to acidic molecules, neutral and basic proteins, *i.e.*, myoglobin (pI = 7.0), human haemoglobin (pI = 7.0), trypsinogen (pI = 9.3) and ribonuclease A (pI = 9.7) were eluted with the first KCl gradient in the double gradient system[a].

The chromatographic behaviours of proteins in a $CaCl_2$ system (in which phosphate ions are absent) were investigated using the KB column with dimensions identical with those for Fig. 2, with the following results. By applying a linear $CaCl_2$ gradient with $g'_{(CaCl_2)}$ (ϕ = 1 cm) = 2.5 mM/ml, ribonuclease A, cytochrome c and chicken lysozyme were eluted at <10 mM, *ca.* 20 mM and <10 mM, respectively; pepsinogen, ovalbumin, BSA, deoxyribonuclease I, myoglobin, bovine haemoglobin and trypsinogen were not eluted at all, even in the presence of 3 M $CaCl_2$. [For the fact

[a] It should be added that the elution molarity, $m_{elu(KCl)}$, of myoglobin in the KCl gradient system is 2.3 times higher than the elution potassium molarity, $m_{elu(K^+)}$, in the KP gradient system under the experimental conditions obtained by using the same L and the same $g'_{(K^+)}$. This means that, although myoglobin behaves as a "basic" molecule in the double gradient system, mainly adsorbed on the **c** surface of HA, it is also partially adsorbed on the **a** surface; the Boltzmann distribution between the two manners of adsorption is not biased extremely towards one of them with this neutral protein. Slight increases in $m_{elu(KCl)}$ (in the KCl system) in comparison with $m_{elu(K^+)}$ (in the KP system) were also observed for human haemoglobin, trypsinogen, ribonuclease A and cytochrome c. This indicates that, even with these neutral or basic proteins, minor proportions of molecules are adsorbed on the crystal surface where acidic molecules should be adsorbed. As far as chicken lysozyme is concerned, however, $m_{elu(KCl)}$ in the KCl system is slightly lower than $m_{elu(K^+)}$ in the KP system (see Fig. 7). This, together with the fact that the shape of the total chromatogram of basic molecules in the KP gradient system is sometimes (slightly) different from that occurring in the KCl gradient system (*e.g.*, compare Fig. 6a with Fig. 6b), would indicate that minor secondary mechanisms (*e.g.*, the change in the molecular conformation depending on the type of the solvent, the interaction mechanism between the sample molecule and ions from the solvent, etc.) interfere in chromatography. It should also be added that the width of a chromatographic peak in the KCl system is sometimes slightly larger than that occurring in the KP system (*e.g.*, compare the double chromatographic peaks of cytochrome c in Fig. 7a with those in Fig. 7b; also compare Fig. 6a with Fig. 6b).

that myoglobin, haemoglobin and trypsinogen (with neutral or basic p*I*), which behaved as "basic" molecules in the KCl system (see above; also see Table 1), behave as "acidic" molecules in the $CaCl_2$ system, see Section 4.1.]

All these data (obtained by using the KB column) are compatible with those obtained by using open columns, leading to the chromatographic mechanism deduced in section 2. For instance, it can be understood from Fig. 7a that the basic molecules (cytochrome *c* and lysozyme) that were adsorbed on one of the two crystal surfaces of HA are first desorbed and developed on the column, driven out of the crystal surface through competition with potassium ions from the first KCl gradient while the acidic molecule (BSA) adsorbed on the other crystal surface remains on the surface; the acidic BSA is hardly affected by the presence of the low molarity (10 m*M*) of KP and by the KCl gradient, as chloride ions are virtually unadsorbable on both of the two types of crystal surface. BSA is desorbed from the HA surface and developed on the column, driven out of the crystal surface through competition with phosphate ions from the second KP gradient. The single KP gradient chromatogram for the same mixture (Fig. 7b) is a superposition of the two chromatograms occurring in parallel on the basis of two different chromatographic mechanisms.

4. TWO TYPES OF ADSORBING SURFACE OF HYDROXYAPATITE AS DEDUCED FROM CRYSTALLOGRAPHY AND ADSORPTION EXPERIMENTS: STEREOCHEMICAL STRUCTURE AND GEOMETRICAL ARRANGEMENT OF ADSORBING SITES ON THE CRYSTAL SURFACE

4.1. Crystallography

HA crystal usually belongs in the space group $P6_3/m$, and the crystal unit cell is characterized by the primitive vectors **a**, **b** and **c** with $\mathbf{a} \wedge \mathbf{b} = 120°$, $\mathbf{a} \wedge \mathbf{c} = \mathbf{b} \wedge \mathbf{c} = 90°$, $|\mathbf{a}| = |\mathbf{b}| = 9.42$ Å and $|\mathbf{c}| = 6.88$ Å (see refs. 31 and 32, but *cf.* ref. 33). In a unit cell of the ideal stoichiometric crystal, ten calcium ions (Ca^{2+}), six phosphate ions (PO_4^{3-}) and two hydroxyl ions (OH^-) are arranged in the manner represented in Fig. 8a. Therefore, the Ca/P molar ratio for the stoichiometric crystal is 1.67.

Fig. 9a–f show scanning electron micrographs of the surface structure of six types of HA particle to be packed in the column for HPLC. The Ca/P molar ratios for the crystals shown are 1.67, 1.67, 1.62, 1.57, 1.52–1.54 and 1.61–1.64, respectively. Therefore, the chemical compositions of the crystals in Fig. 9a and b are stoichiometric with respect to both calcium and phosphorus; the crystal structures of HA in Figs. 9c–f involve some defects.

The surface structure shown in Fig. 9a is quasi-ideal, and it can be identified that an HA particle is an aggregate of hexagonal rods each representing a crystallite or a micro-monocrystal. It can also be identified that the cross-sectional surface of a rod, hexagonal in shape, is an (001) surface or a **c** surface which is parallel to the (**a**, **b**) plane of the crystal unit cell; the six surfaces, rectangular in shape, occurring around the main axis of the rod are (100) or (010) surfaces, *i.e.*, **a** or **b** surfaces. These are parallel to the (**b**, **c**) or the (**a**, **c**) plane of the crystal unit cell (see Fig. 8a). (The **a** and the **b** surfaces are equivalent to each other. Hereafter, except in certain instances, we call both **a** and **b** surfaces simply an **a** surface.) Thus, on a polycrystal of the type shown in Fig. 9a, only **a** and **c** surfaces appear; the total area of the **c** surfaces is much smaller than that of the **a** surfaces.

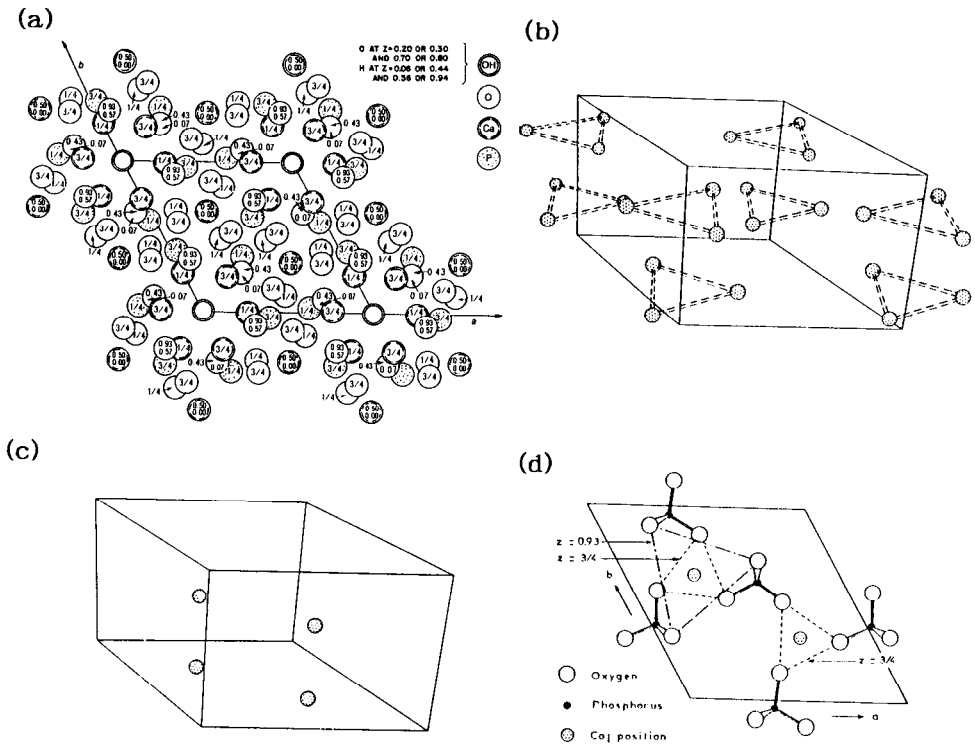

Fig. 8. (a) HA structure projected on the (**a**, **b**) plane along the **c** axis which is vertical to the plane of the paper. The parallelogram represents a crystal unit cell. The numerical values on the atoms represent z values *i.e.*, coordinates along the **c** axis; $z = 0$ and 1 at the lower and the upper margin of a unit cell, respectively. Calcium ions at $z = 0.00$ and $z = 0.50$ are called Ca_I ions, and those at $z = 1/4$ and $z = 3/4$ are called Ca_{II} ions. (Reproduced with slight modifications from ref. 31.) (b) Perspective view of Ca_{II} ions. The outline of the crystal unit cell is also drawn, where **a** is horizontally directed to the right in the plane of the paper, **b** is directed into the paper and **c** is vertical and upwards. It can be seen that there are a pair of triangular arrays of Ca_{II} ions centred on each edge (6_3 axis) of the unit cell, which lie on two mirror planes [parallel to the (**a**, **b**) plane] being at levels of $z = 1/4$ and $z = 3/4$, respectively. A pair of hydroxyl ions are also centred on each 6_3 axis, surrounded by the pair of triangular arrays of Ca_{II} ions, respectively. [Hydroxyl ions are not drawn; for the z values for the ions, see (a).] When the ($\mathbf{a} = \mathbf{0}, \mathbf{c} = \mathbf{0}$) or the ($\mathbf{b} = \mathbf{0}, \mathbf{c} = \mathbf{0}$) plane of the unit cell is on the crystal surface, one of the three Ca_{II} ions constituting a triangular array is outside the crystal; the two other Ca_{II} ions survive on the crystal surface, receding slightly behind the ($\mathbf{a} = \mathbf{0}, \mathbf{c} = \mathbf{0}$) or the ($\mathbf{b} = \mathbf{0}, \mathbf{c} = \mathbf{0}$) plane. It can be deduced that, when the HA crystal is suspended in an aqueous solution, the hydroxyl positions on the crystal surface, each inserted by two Ca_{II} ions, are void at least for an instant. (Reproduced from ref. 34. The above interpretation was given in ref. 35, however.) (c) Perspective view of Ca_I ions. It can be seen that there are two columns of Ca_I ions per unit cell along two three-fold rotatory symmetry axes, and that each column is constituted of two Ca_I ions occurring at $z = 0.00$ and $z = 0.50$ (nearly, but not precisely, at $z = 0$ and $z = 1/2$, respectively). (Reproduced from ref. 34.) (d) Deduced structure of the **c** surface of HA. It can be deduced that, when the HA crystal is suspended in an aqueous solution, two types of Ca_I position appearing on the **c** surface of HA are void at least for an instant. One of them is surrounded by six oxygen atoms (upper left) and the other by three oxygen atoms (lower right). (Reproduced from ref. 36.)

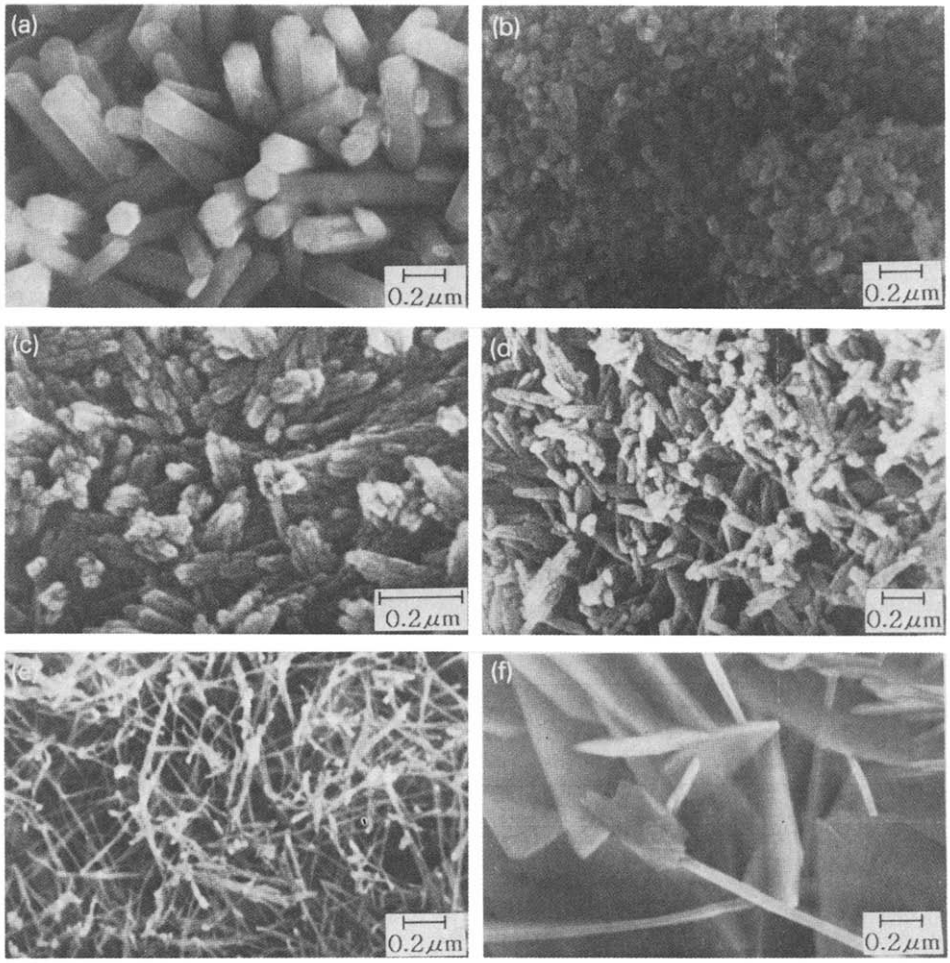

Fig. 9. Scanning electron micrographs of the surface structure of (a) coral HA with a Ca/P molar ratio of 1.67 (Mitsui Toatsu Chemicals), (b) spherical HA type S with a Ca/P molar ratio of 1.67 (Koken), (c) HA type H with a Ca/P molar ratio of 1.62 (Koken), (d) HA type F with a Ca/P molar ratio of 1.57 (Koken), (e) potato-like HA with a Ca/P molar ratio of 1.52–1.54 (Central Glass) and (f) "rose des sables"-like HA with a Ca/P molar ratio of 1.61–1.64 (Central Glass). The entire image of HA type S (b) is shown in Fig. 1. HA type H (c) is the Tiselius-type HA with a plate-like entire external shape. HA type F (d) has a square tile-like entire shape. The name "potato-like HA" (e) arises from the entire image of the crystal. "Rose des sables" (f) is a French word representing a gypsum flower produced naturally in the Sahara Desert. (Reproduced from ref. 37.)

The HA shown in Fig. 9e is an aggregate of micro-crystals with a needle-like shape. From the crystal habit, it is highly probable that the **c** axis is parallel to the main axis of the "needle", and that most of the crystal surfaces appearing around the main axis of the "needle" are **a** surfaces.

Monma *et al.* [38] performed an electron diffraction analysis of an HA crystal with an external shape very similar to that of "rose des sables"-like HA, the surface of

which is covered with lamellae (Fig. 9f). They reported [38] that the flat surface of a lamella corresponds to the (100) or the **a** surface as deduced from the electron diffraction pattern. It is therefore highly probable that the flat surface of a lamella of "rose des sables"-like HA also corresponds to the **a** surface, and that the major proportion of the total surface of the lamella is occupied by the **a** surface. Non-lamellar structures can also be found on the crystal surface of "rose des sables"-like HA by carefully exploring the electron micrograph, however.

With regard to the other crystals shown in Fig. 9b–d, it is difficult to identify the crystal surface on the basis of the electron micrograph only.

A comparative study of the crystal structure of HA with that of octacalcium phosphate (OCP) [39,40] in combination with a study of the degradation mechanism of polyphosphates occurring on the crystal surface of HA [40,41] leads to the deduction that the **a** (or **b**) surface which just intersects the **b** (or **a**) axis of the crystal unit cell (see Fig. 8a), in fact appears on an HA crystal [35,40]. This means that positions at which hydroxyl ions should be present, provided the positions are situated in the interior of the crystal, appear on the crystal surface, inserted by two Ca_{II} ions (see Fig. 8b; *cf.*, Fig. 8a). It can be deduced [35,40] that, when the HA crystal is suspended in an aqueous solution, the hydroxyl positions on the crystal surface, each inserted by two Ca_{II} ions, are void at least for an instant, and that the two Ca_{II} ions (with positive charges) constitute an adsorbing site (see Fig. 8b). It can further be deduced [35] that the site is identical with the chromatographic C site, or the anion exchanger on which a competing phosphate ion from the phosphate buffer and a phosphate or a carboxyl group on the sample macromolecule are adsorbable (see section 2). (A free phosphate ion and a phosphate group on the macromolecule would be adsorbed directly on a hydroxyl position [35,40]. The possibility cannot be excluded, however, that a carboxyl group on the macromolecule is adsorbed on a position situated in the middle of two hydroxyl positions arranged in the **c** direction on the **a** surface of HA. This is because carbonic ions may be situated at corresponding positions in the interior of the crystal, excluding hydroxyl ions [34].) A picture can finally be obtained that, on the **a** (or **b**) surface of HA, adsorbing C sites are arranged in a rectangular manner with an inter-site distance in the **b** (or **a**) direction equal to $|\mathbf{b}|$ ($= |\mathbf{a}|$) $= 9.42$ Å and an inter-site distance in the **c** direction equal to $|\mathbf{c}|/2 = 3.44$ Å (*cf.*, Fig. 8b).

The mechanism of the adsorption of both free ions and adsorption groups of macromolecules on the crystal surface of HA resembles the first step of the epitaxial growth of the crystal (see ref. 36, Appendix II), where epitaxy consists in the growth of one crystal, in one or more particular orientations, on a substrate of another, with a near geometrical fit between the respective networks that are in contact [42]. In fact, if hydroxyl positions (C sites) on the **a** surface of HA are filled, under certain circumstances, with hydroxyl ions, then the crystal growth of HA would continue [35,40]. If hydroxyl positions are filled in an alternate manner with both phosphate ions and water molecules, then the epitaxial growth of OCP might begin on the **a** surface of HA [35,40].

It can be deduced that the **c** surface of HA is situated at the level of $z = 0.00$ or $z = 0.50$ as the exposure of another level of z on the crystal surface is only possible in compensation for the destruction of the chemical structure of crystal phosphate ions (see ref. 36, Appendix II). The levels $z = 0.00$ and $z = 0.50$, which are equivalent to each other, are those where Ca_I ions should be present, provided that the levels are

situated in the interior of the HA crystal (see Fig. 8c; *cf.*, Fig. 8a). It can be deduced [36] that, when the HA crystal is suspended in an aqueous solution, the Ca_I positions on the crystal surface are void at least for an instant; two types of Ca_I position appear on the **c** surface of HA, one surrounded by six negatively charged oxygen atoms belonging to three crystal phosphates and the other surrounded by three negatively charged oxygen atoms belonging to three crystal phosphates (see Fig. 8d). It can be assumed [36] that the former Ca_I position is identical with the chromatographic P site, or the cation exchanger on which a competing sodium or potassium ion from the buffer and an ε-amino or a guanidinyl group on the protein molecule are adsorbable (see Section 2); the latter Ca_I position may constitute a weak adsorbing site. A picture can finally be obtained that, on the **c** surface of HA, adsorbing P sites are arranged in a hexagonal manner with the minimum inter-site distance in both **a** and **b** directions equal to $|\mathbf{a}| = |\mathbf{b}| = 9.42$ Å.

Of course, the possibility cannot be excluded that, owing to surface tension, the stereochemical structures of both **a** and **c** surfaces are distorted to a certain extent in comparison with the structure occurring in the interior of the crystal. It can be assumed, however, that the surface structure that has been deduced above represents the true structure to a good approximation.

The chromatographic behaviour of proteins as a function of p*I* in the $CaCl_2$ system is fundamentally almost parallel with the behaviour in the KCl system (*cf.*, 14th column in Table 1). Myoglobin, haemoglobin and trypsinogen, which behave as "basic" molecules in the KCl system, behave as "acidic" molecules in the $CaCl_2$ system, however (see Section 3 and also Table 1). Further, the adsorption of "acidic" proteins on the HA surface is generally stabilized in the presence of calcium ions in the mobile phase (see Section 2). It can be suggested that, once a carboxyl group of the molecule has been adsorbed on a C site constructed from two crystal calcium ions (see above), a calcium ion from the mobile phase is also fixed on the C site, completing a triangular array of calcium ions around the carboxyl group (*cf.*, Fig. 8b). The structure constructed from three calcium ions and a carboxyl group would resemble the corresponding structure in the interior of the crystal occurring when one (or two) hydroxyl ion(s) is (are) replaced with a carbonic ion (see above). On the basis of this mechanism, the adsorption of a carboxyl group on a C site would be stabilized in the presence of calcium ions in the mobile phase. It can also be suggested that the behaviours of myoglobin, haemoglobin and trypsinogen as "acidic" molecules in the presence of calcium ions in the mobile phase (see above) are intimately related to this adsorption mechanism.

4.2. Adsorption experiments: direct experimental confirmation of the existence of two types of adsorbing surface, **a** *and* **c**

The adsorption experiments on proteins were carried out as follows. By using the same method as in HPLC, the sample molecules dissolved in a 1 m*M* KP buffer were injected into a column; this was followed by a rinsing process carried out by using 1 m*M* KP buffer. The column contents (*i.e.*, HA particles) were extruded from the inlet of the column by pushing them from the outlet with a rod. The cylindrical mass of the HA particles extruded from the column was cut into slices of thickness 2 mm; each of them was then suspended in 0.5 *M* KP with agitation in order to dissolve the sample molecules that had been captured on HA surfaces. The suspension was centrifuged and

the absorbance of the supernatant was measured in order to calculate the total amount of the sample molecules that had been present in the slice [37].

The histograms in Fig. 10 show typical examples of the adsorptions of BSA (with an acidic p*I* of 4.7) and chicken lysozyme (with a basic p*I* of 10.5–11.0) obtained in the presence of 1 m*M* KP. These are drawn as functions of the distance, *L*, from the inlet of the columns packed with six different types of HA (Fig. 9); the amount of molecules involved in a 2-mm slice of the column contents is represented by a portion of the histogram with a width of 2 mm. Hence the histograms in Fig. 10a–f represent those for BSA obtained by using columns packed with coral HA (Fig. 9a), HA type S (Fig. 9b), HA type H (Fig. 9c), HA type F (Fig. 9d), potato-like HA (Fig. 9e) and "rose des sables"-like HA (Fig. 9f), respectively. The histograms in Fig. 10a′–f′ are for lysozyme, corresponding to those in Fig. 10a–f. It can be seen in Fig. 10 that, with both coral HA (constructed with hexagonal rods) and potato-like HA (constructed with "needles"), the mean height of the histogram (m.h.h.) for basic lysozyme is much smaller than that for acidic BSA (*cf.*, parts a and a′ and parts e and e′, respectively). With these two types

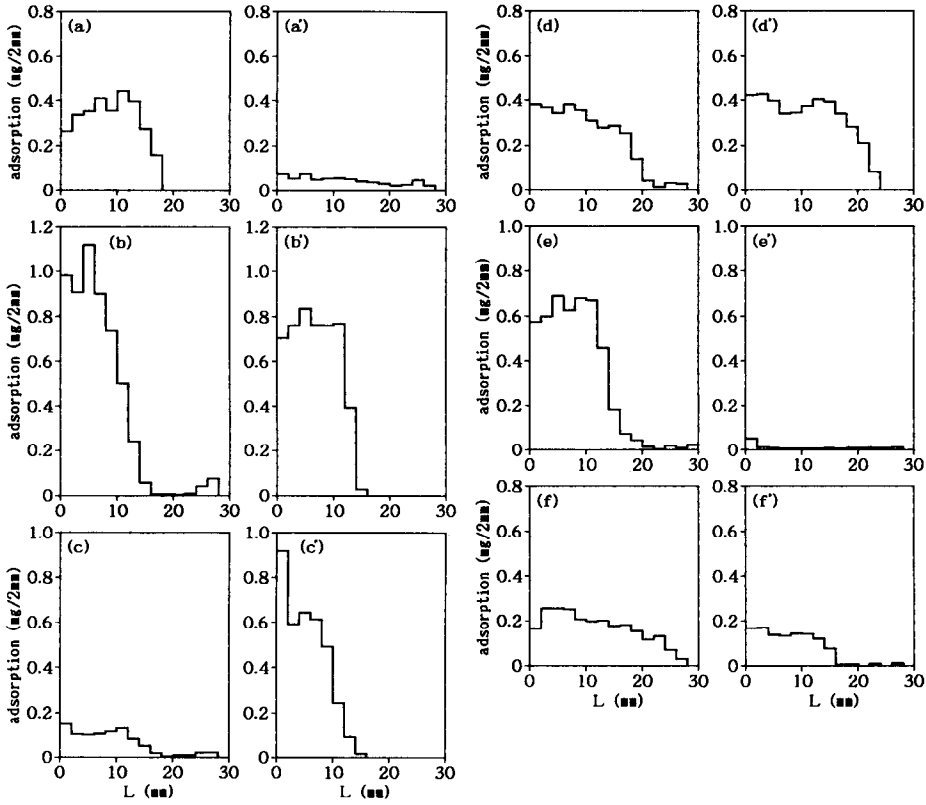

Fig. 10. Amounts of BSA (a–f) and chicken lysozyme (a′–f′) adsorbed per 2-mm slice of the column contents (with ϕ = 6 mm) in the presence of 1 m*M* KP as functions of the distance, *L*, from the column inlet. Types of the crystal packed in the column are coral HA for (a) and (a′), HA type S for (b) and (b′), HA type H for (c) and (c′), HA type F for (d) and (d′), potato-like HA for (e) and (e′) and "rose des sables"-like HA for (f) and (f′). (Reproduced from ref. 37.)

of HA, the total area of the **c** surface is much smaller than that of the **a** surface (section 4.1), and it can be confirmed that lysozyme (with a basic p*I*) is adsorbed (mainly; see the second footnote in Section 3) on the **c** surface whereas BSA (with an acidic p*I*) is adsorbed (mainly) on the **a** surface. [It is highly probable that the major proportion of the total surface of the lamella of "rose des sables"-like HA is occupied by the **a** surface (Section 4.1). With this HA, however, the m.h.h. for lysozyme is only slightly smaller than that for BSA (Fig. 10f and f'). This probably arises from the coexistence of the non-lamellar structure; see Section 4.1.]

By using a method similar to that used for both lysozyme and BSA, it was confirmed [37] that other neutral and basic proteins, *i.e.*, myoglobin (p*I* = 7.0),

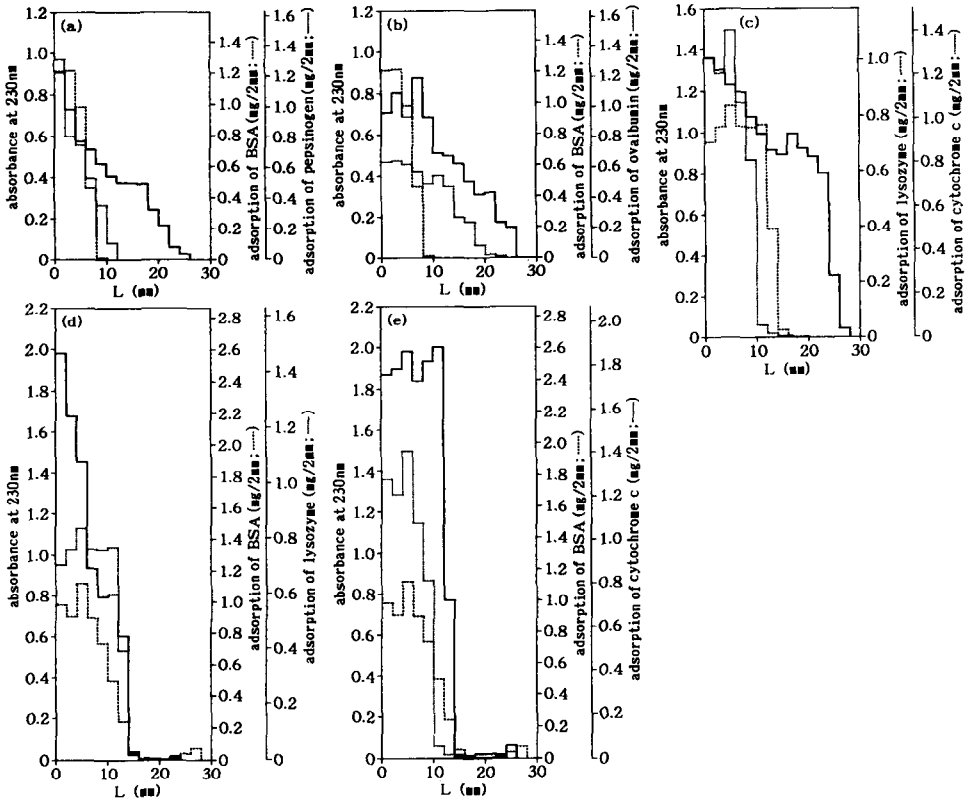

Fig. 11. As Fig. 10, obtained in the presence of 1 m*M* KP by using the column packed with HA type S for mixtures of (a) BSA and pepsinogen, (b) BSA and ovalbumin, (c) lysozyme (chicken) and cytochrome *c*, (d) BSA and lysozyme (chicken) and (e) BSA and cytochrome *c*. (The histograms for the mixtures are drawn with a continuous line.) Independent histograms for the respective components of the mixture are also drawn, where the amounts of the components are equal to those appearing in the mixture. [The independent histograms are drawn with two types of dotted line. Independent histograms for lysozyme in (c), BSA in (d), lysozyme in (d) and BSA in (e) have been reproduced from Fig. 10b', 10b, 10b' and 10b, respectively.] On the left-hand ordinate, the absorbance at 230 nm of the supernatant is indicated instead of the amount of molecules adsorbed per 2-mm slice of the column contents (see the introductory part of this section). These amounts for the respective components of the mixture in the independent histograms are indicated on the right-hand ordinate. (Reproduced from ref. 37.)

trypsinogen (pI = 9.3), ribonuclease A (pI = 9.7) and cytochrome c (pI = 9.8–10.0), are adsorbed (mainly) on the **c** surface. Other acidic proteins, *i.e.*, pepsinogen (pI = 3.9) and ovalbumin (pI = 4.6), are adsorbed (mainly) on the **a** surface. (For details, see ref. 37.)

The histograms in Fig. 11 were obtained in the presence of 1 mM KP by using columns packed with HA type S for several types of protein mixture. In Fig. 11, independent histograms for the respective components of the mixture are also drawn, where the amounts of the components are equal to those appearing in the mixture. Thus, Fig. 11a and b are concerned with mixtures of acidic proteins, *i.e.*, a mixture of BSA and pepsinogen and a mixture of BSA and ovalbumin, respectively. Fig. 11c is for a mixture of basic proteins, lysozyme (chicken) and cytochrome c. Fig. 11d and e are concerned with mixtures of acidic and basic proteins, *i.e.*, a mixture of BSA and lysozyme (chicken) and a mixture of BSA and cytrochrome c, respectively. It can be seen in Fig. 11 that, with both the mixture of acidic proteins [(a) and (b)] and the mixture of basic proteins (c), the width of the total histogram is roughly equal to the sum of the widths of the independent histograms for the respective components. With the mixtures of acidic and basic proteins, however, the height of the total histogram is roughly equal to the sum of the heights of the independent histograms for the respective components (see Fig. 11d and e). These data indicate that acidic proteins are adsorbed on a common surface of HA, and that basic proteins are also adsorbed on a common surface; acidic and basic proteins are adsorbed on different crystal surfaces of HA.

4.3. Relationship with HPLC

By using the double gradient technique (Section 3), it can be confirmed [37] that, with respect to all the six types of HA (Fig. 9), acidic proteins (pepsinogen, ovalbumin, BSA and β-lactogloblin A) are eluted with the second KP gradient whereas basic and neutral proteins (myoglobin, trypsinogen, ribonuclease A, cytochrome c and chicken lysozyme) are eluted with the first KCl gradient.

The points in Fig. 12a–f are experimental plots of $m_{\mathrm{elu(P)}}$ *versus* pI for the above proteins, obtained by using columns packed with (a) coral HA, (b) HA type S, (c) HA type H, (d) HA type F, (e) potato-like HA and (f) "rose des sables"-like HA; a single KP gradient was used for the development of the proteins. (The plots for pepsinogen, ovalbumin, myoglobin, trypsinogen and ribonuclease A are concerned with the main peak of the chromatogram.) In all the experiments, the total length, L, of the column was fixed at 13 cm and the slope $g'_{\mathrm{(P)}}$ (ϕ = 1 cm) = 2.5 mM/ml of the KP gradient was applied. It can be seen in Fig. 12 that, in general, "acidic" proteins tend to be eluted at lower phosphate molarities than "basic" proteins while maintaining almost the same constellations of the plot among the "acidic" and the "basic" proteins, respectively. With coral HA, potato-like HA and "rose des sables"-like HA, however, the elution molarities of the "basic" proteins tend to decrease; as a result, the elution molarities of the "acidic" proteins and those of the "basic" proteins tend to approach each other (compare Fig. 12a, e and f with Fig. 12b, c and d).

The fact that the constellation of the $m_{\mathrm{elu(P)}}$ *versus* pI plot among the acidic proteins and the constellation of the same plot among the basic (and neutral) proteins are both almost parallel among all the HAs with different external shapes (Fig. 12) indicates that the two common active surfaces (**a** and **c**) appear independently of the

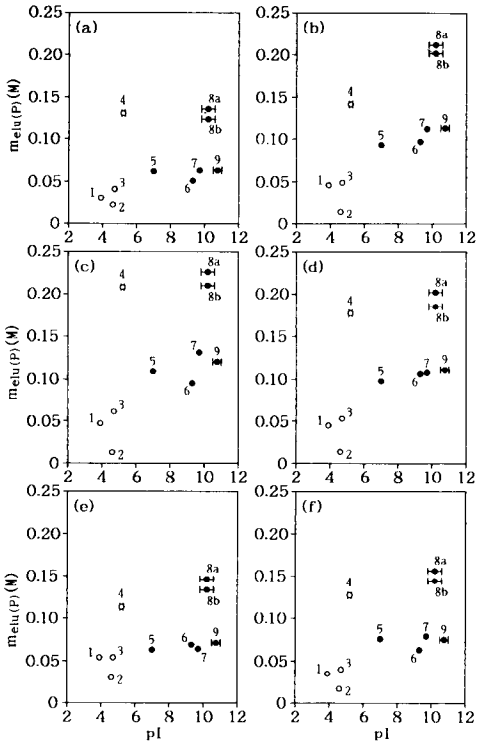

Fig. 12. Plots of $m_{elu(P)}$ *versus* p*I* for (1) pepsinogen, (2) ovalbumin, (3) BSA, (4) β-lactoglobulin A, (5) myoglobin, (6) trypsinogen, (7) ribonuclease A, (8a) cytochrome *c* in the reduced state, (8b) cytochrome *c* in the oxidized state and (9) chicken lysozyme, obtained by using columns packed with (a) coral HA, (b) HA type S, (c) HA type H, (d) HA type F, (e) potato-like HA and (f) "rose des sables"-like HA; ○ and ● indicate "acidic" and "basic" molecules, respectively. In all the experiments, the column with dimensions ϕ = 6 mm and L = 13 cm was used, and the slope, $g'_{(P)}$ (ϕ = 1 cm) = 2.5 mM/ml, of the KP gradient was applied. The two points (8a and 8b) for cytochrome *c* in (a) were obtained from interpolation by using theoretical curves, however (*cf.*, Fig. 13a, where the theoretical curve for cytochrome *c* in the reduced state is drawn). Other experimental conditions: (a) sample load = 30–100 μg, flow-rate = 0.50 ml/min, P = 1.5–4.0 MPa, T = 24.5–26.5°C; (b) sample load = 25–300 μg, flow-rate = 0.49–0.51 ml/min, P = 1.3–2.4 MPa, T = 23.2–29.7°C; (c) sample load = 30–400 μg, flow-rate = 0.50–1.01 ml/min, $P \leqslant$ 0.2 MPa, T = 24.5–27.0°C; (d) sample load = 10–275 μg, flow-rate = 0.50–1.01 ml/min, P = 0.2–0.5 MPa, T = 24.5–27.0°C; (e) sample load = 35–90 μg, flow-rate = 0.50–0.51 ml/min, $P \leqslant$ 0.2 MPa, T = 24.0–26.0°C; (f) sample load = 28–94 μg, flow-rate = 0.50–0.51 ml/min, $P \leqslant$ 0.2 MPa, T = 23.0–26.2°C. (Reproduced from ref. 37.)

external crystal shape of HA. Further, the fact that the elution molarity of the basic proteins tends to decrease in comparison with that of the acidic proteins in the case of three types of HA (coral HA, potato-like HA and "rose des sables"-like HA) can be explained on the basis of the chromatographic theory by assuming that the active surface for basic proteins (*i.e.*, the **c** surface) is much smaller than that for acidic proteins (*i.e.*, the **a** surface) for these HA [37] (*cf.*, section 7).

The points in Fig. 13a–f are experimental plots of $m_{elu(P)}$ *versus* ln $s_{app(P)}$ for BSA, chicken lysozyme and cytochrome *c* in the reduced state, obtained by using columns

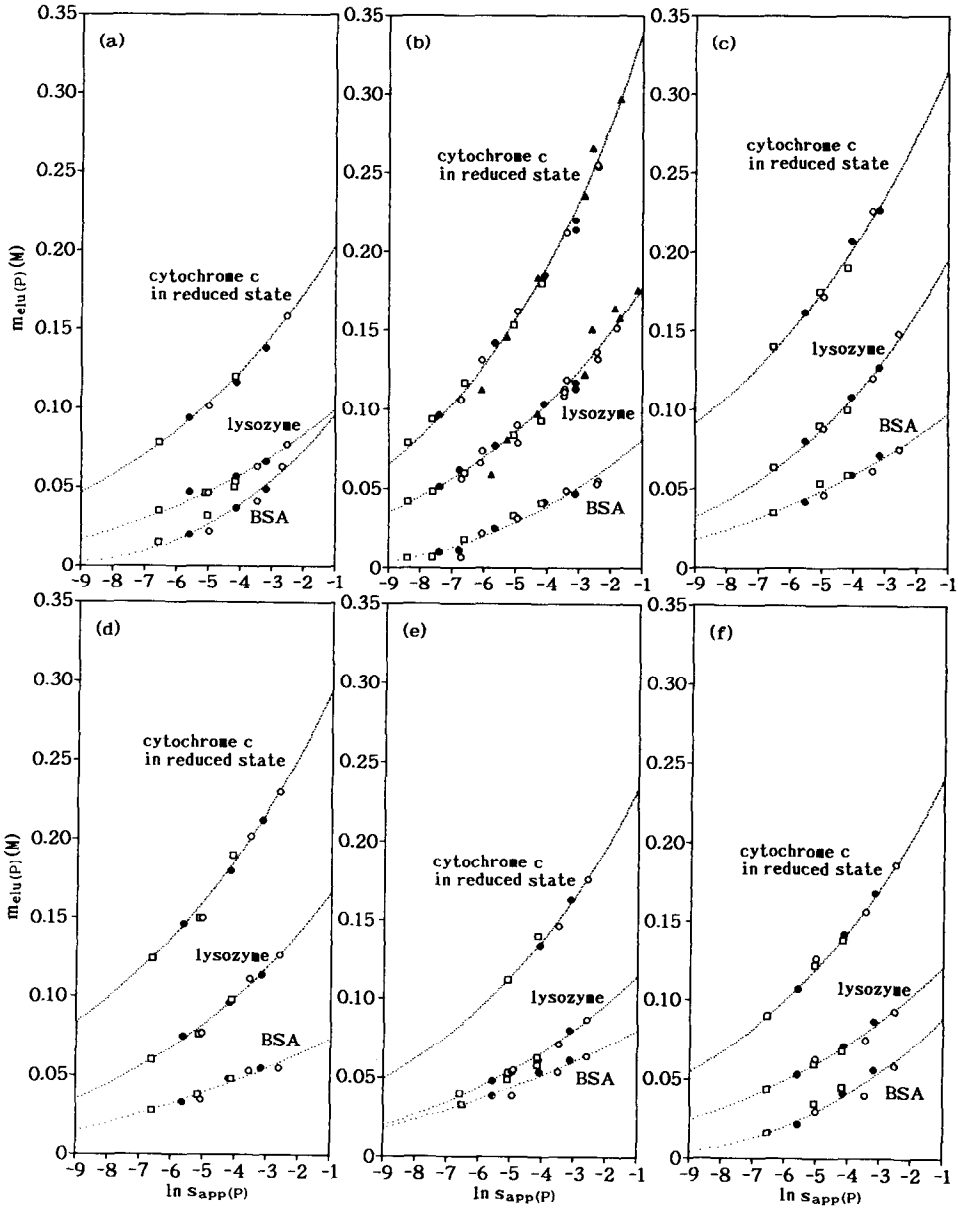

Fig. 13. Points: experimental plots of $m_{elu(P)}$ *versus* ln $s_{app(P)}$ for BSA, chicken lysozyme and cytochrome *c* in the reduced state, obtained by using columns packed with (a) coral HA, (b) HA type S, (c) HA type H, (d) HA type F, (e) potato-like HA and (f) "rose des sables"-like HA; ϕ is always equal to 6 mm. The $g'_{(P)}$ (ϕ = 1 cm) values that were applied are (▲) 5.0, (○) 2.5, (●) 1.25 and (□) 0.45 m*M*/ml. Other experimental conditions: (a) sample load = 30–150 μg, flow-rate = 0.46–0.52 ml/min, P = 0.1–0.6 MPa, T = 21.0–29.7°C; (b) sample load = 16–480 μg, flow-rate = 0.46–0.51 ml/min, P = 0.3–10.0 MPa, T = 21.0–29.7°C; (c) sample load = 30–200 μg, flow-rate = 0.50–0.51 ml/min, $P \leqslant 0.4$ MPa, T = 23.8–25.1°C; (d) sample load = 30–150 μg, flow-rate = 0.50 ml/min, P = 0.2–0.6 MPa, T = 23.0–26.0°C; (e) sample load = 27–150 μg, flow-rate = 0.50–0.51 ml/min, $P \leqslant 0.2$ MPa, T = 23.3–27.0°C; (f) sample load = 28–145 μg, flow-rate = 0.50–0.51 ml/min, $P \leqslant 0.2$ MPa, T = 23.5–27.0°C. Curves: theoretical curves calculated by using eqn. 14 in section 7. (Reproduced from ref. 37.)

packed with (a) coral HA, (b) HA type S, (c) HA type H, (d) HA type F, (e) potato-like HA and (f) "rose des sables"-like HA, where $s_{app(P)}$ is the product of the slope, $g'_{(P)}$ (ϕ = 1 cm), of the molarity gradient and the total length, L, of the column. The curves in Fig. 13 are theoretical, calculated by using eqn. 14 in Section 7. [For details of the $m_{elu(P)}$ *versus* ln $s_{app(P)}$ plot, see section 7.] It can be seen in Fig. 13 that, with coral HA (a), potato-like HA (e) and "rose des sables"-like HA (f), the elution molarities of "basic" proteins, lysozyme and cytochrome *c*, tend to decrease, and that they approach those of "acidic" BSA; especially the elution molarities of lysozyme are close to those of BSA.

Finally, it should be pointed out that the **a** surface of some commercially available spherical HA particles is damaged to a considerable extent. With these particles, acidic proteins are adsorbed so weakly on the **a** surface that the molecules are eluted from the column even before the second KP gradient begins in the double gradient system. In our experience, it is highly probable that the destruction of the surface structure occurred at least partially in the sintering process of micro-crystals to make up a sphere.

5. SEPARATION OF PROTEIN MOLECULES WITH SUBTLE STRUCTURAL DIFFERENCES

A molecule, in general, can take a number of different adsorption configurations on the crystal surface of HA. In other words, the molecule can be adsorbed using a number of different local molecular surfaces, each of which can face the crystal surface and can orient in different directions on the crystal surface. Following a statistical-mechanical law, a Boltzmann distribution is realized among the configurations, and the energetically most stable adsorption configuration is realized in the highest probability (see eqn. 7 in section 7). In other words, the stereochemical structure of the local molecular surface (facing the crystal surface when the molecule is in the energetically most stable configuration) can be recognized by the regularity of the crystal surface structure of HA. As a result, the molecular separation highly characteristic of HA chromatography is realizable.

In contrast to HA chromatography, in the usual ion-exchange chromatography the geometrical arrangement of the adsorbing sites (called ion exchangers) on the adsorbent would fluctuate microscopically among different loci in the column, as the adsorbing sites are part of an organic substrate with a more or less flexible stereochemical structure. This implies that the energetically most stable configuration of a protein molecule adsorbed on the organic substrate varies among different loci in the column, and that the charges on the total molecular surface are used fairly uniformly for the reaction with the adsorbent throughout a development process on the column. (In the usual reversed-phase chromatography also, the adsorbing sites are part of an organic substrate with a flexible structure. It can be suggested, therefore, that the hydrophobic structures on the total molecular surface are used fairly uniformly for the reaction with the adsorbent.) HA chromatography resembles affinity chromatography in that a subtle difference in the geometrical arrangement of atoms on a local molecular surface may be discriminated by the column owing to the regular stereochemical structure of the adsorbent surface.

It can be seen in Fig. 12 that acidic proteins tend to be eluted at lower phosphate molarities than basic proteins. It should be emphasized, however, that among the

"acidic" and "basic" proteins (*i.e.*, among the proteins obeying the same chromatographic mechanism), the correlation between $m_{elu(P)}$ and p*I* is very weak. (A similar experimental plot can be obtained by using the data represented in Table 1; see Fig. 2 in ref. 30.)

The points in Fig. 14 are experimental plots (reproduced from ref. 43) of p*I* *versus* elution (or retention) time for a number of proteins obtained with an anion-exchange HPLC column where a linear NaCl gradient has been applied; the elution molarity, in general, increases linearly with increase in elution time. It can be seen in Fig. 14 that elution time (*i.e.*, elution molarity) is strongly correlated with p*I*.

Both Figs. 12 and 14 firmly support the deduction (see above) that the HA column discerns a stereochemical structure on a local surface of a protein molecule whereas the ion-exchange column is sensitive to the total charge per molecule. (The possibility cannot be excluded, however, that, under certain circumstances where the secondary or the tertiary structure of the molecules under examination is fluctuating to a larger extent, a stronger correlation may be realized between p*I* and elution molarity even in HA chromatography. In the special case when only the local molecular surface interfering in the reaction with the HA surface varies among the molecules under examination, a strong correlation might also be realized between p*I* and elution molarity.)

Fig. 15 illustrates a typical example of the chromatographic separation of four molecular species of human tumour necrosis factor (h-TNF) proteins with subtle structural differences from one another, obtained on an HA column by using a linear NaP gradient. An h-TNF protein is constructed by aggregation of three subunits. These involve two types, one containing a polypeptide chain of 157 amino residues with amino-terminal valine, and the other containing a polypeptide chain of 158 amino residues, occurring by addition of a methionine to the terminal valine residue. As a result, four types of trimer or four species of h-TNF protein are produced; these involve (1) that constructed with only the latter type of subunit, (2) that constructed with both the latter and the former type of subunits with a ratio of 2:1, (3) that constructed with both types of subunit with a ratio of 1:2 and (4) that constructed with

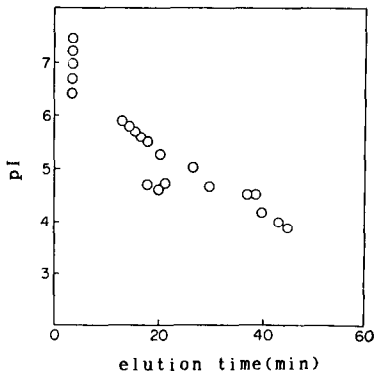

Fig. 14. Plots of p*I* *versus* elution time for a number of proteins obtained with an anion-exchange DEAE-5PW column of dimensions 10 × 0.78 cm I.D. (Tosoh); a linear NaCl gradient (0–0.4 *M*) was applied in the presence of 50 m*M* Tris–HCl buffer at pH 7.5. (Reproduced from ref. 43.)

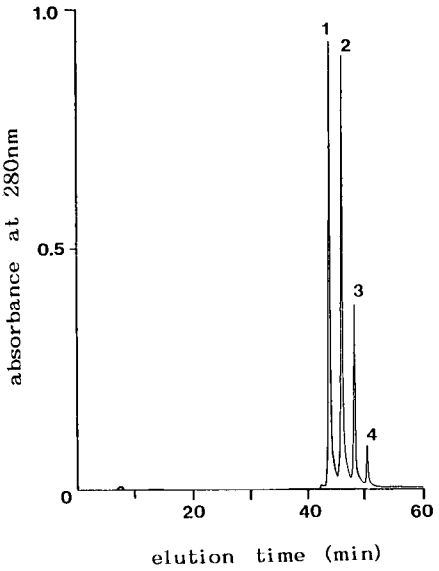

Fig. 15. Chromatographic separation of four molecular species of human tumour necrosis factor obtained on an HPLC column packed with spherical HA (Tonen). Column dimensions ϕ = 7.5 mm and L = 10 cm, and a linear NaP gradient from 10 to 400 mM was applied in 60 min with a flow-rate of 0.5 ml/min. (The chromatogram, published in ref. 44, is presented here by courtesy of Dr. K. Inaka, Protein Engineering Research Institute, Osaka, Japan.)

only the former type of subunit. The four chromatographic peaks marked 1, 2, 3 and 4 in Fig. 15 represent these four h-TNF species in that order. It was confirmed [44] that the h-TNF protein gives only a single band in electrophoresis on polyacrylamide gel carried out in both the absence and the presence of sodium dodecyl sulphate. The protein also gave a single peak in gel, ion-exchange and reversed-phase HPLC [44].

It can be expected, in general, that the HA column will display a specific ability if it is used in the final step of the purification. The sample may be revealed to be still heterogeneous even though it appeared to be homogeneous according to other analytical methods, including chromatography.

6. HYDROXYAPATITE HPLC IN AN ORGANIC SOLVENT SYSTEM

The separation of a variety of glycosides of tri- and diterpenes including *Ginseng* saponins and *Stevia* sweet glycosides can be achieved on an HA column by using an aqueous acetonitrile system [22]. Fig. 16 illustrates typical examples of the chromatographic separation of saponins of *Panax ginseng*, obtained on an HA column in the presence of (a) 80% aqueous acetonitrile and (b) a linear gradient from 90% to 70% aqueous acetonitrile. It can be deduced [45–47] that the adsorption and desorption mechanism occurring in the presence of acetonitrile is different from that involved in the usual aqueous system both in the absence of acetonitrile and in the presence of the inorganic salt.

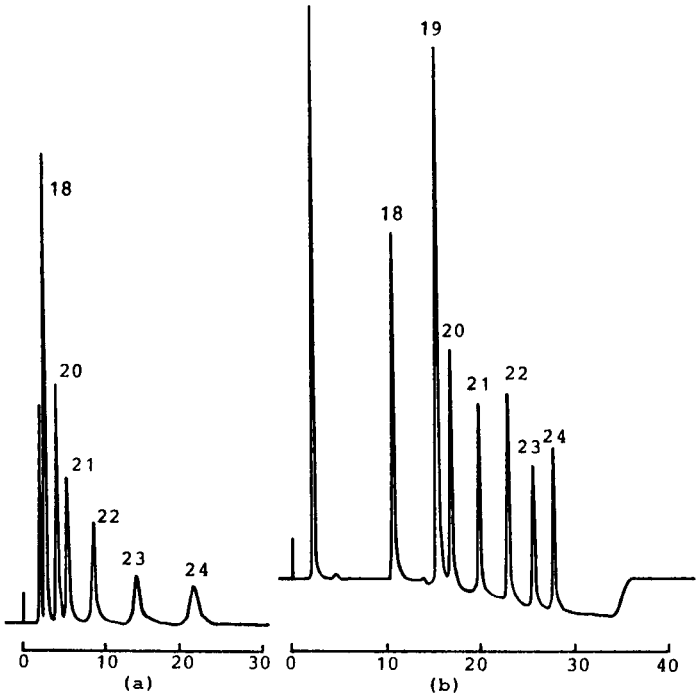

Fig. 16. Chromatographic separations of saponins of *Panax ginseng* obtained on an HPLC column packed with spherical HA (Asahi Optical). Column dimensions ϕ = 7.5 mm and L = 10 cm, and chromatography was carried out in the presence of (a) 80% aqueous acetonitrile and (b) a linear gradient from 90% to 70% aqueous acetonitrile in 30 min. (Reproduced from ref. 22.) Time scale in min.

7. GENERAL THEORY OF LINEAR GRADIENT CHROMATOGRAPHY *VERSUS* HYDROXYAPATITE HPLC

7.1. General theory

A general theory of linear gradient chromatography has been developed with an intimate relationship with the study of HA chromatography. This involves (a) the quantitative study of the adsorption and desorption phenomena occurring in the column [45–49] and (b) the quantitative study of the role of the molarity gradient [50–55].

With regard to study (a), a competition model was introduced [45–49]. The model is compatible with the deductions made in Section 2, and it states that adsorbing sites are arranged in some manner on the surfaces of the packed particles (HA crystals) in the column; the sample molecules (with adsorption groups) and a gradient element (*i.e.*, competing ions from the gradient; see Sections 2 and 3) compete for adsorption on the sites of the packed particles.

Under small load conditions, the molecular bands of each component of the sample mixture migrate independently of one another from the inlet to the outlet of the column while attaining an apparent thermodynamic equilibrium between the mobile and the stationary phase at least at the mean part (usually the centre) of the band; at

this part, the partition, B, of molecules in the mobile phase is equal to the relative migration rate, R_F, *i.e.*, the ratio of the migration rate of molecules to that of the carrier solvent (first principle of chromatography; see ref. 51, Appendix III). On the basis of the competition model, the partition, B, in the equilibrium state can be written as

$$B = \frac{1}{1 + q(\varphi m + 1)^{-x'}} \tag{1}$$

or the capacity factor k' [$\equiv(1 - B)/B$] can be represented as

$$k' = q(\varphi m + 1)^{-x'} \tag{2}$$

where m represents the molarity of competing ions (from the gradient) and x', in general, represents approximately the number of competing ions the adsorption of which on the adsorbent surface is impossible owing to the presence of an adsorbed sample molecule. Therefore, provided that a single adsorbing site is covered by a competing ion when it is adsorbed, x' represents the number of sites on which the adsorption of competing ions is impossible owing to the presence of an adsorbed molecule, *i.e.*, the number of sites that are covered by an adsorbed sample molecule. φ is virtually a positive constant almost proportional to the factor $\exp(\dot{\varepsilon}/kT)$, where $-\dot{\varepsilon}(\dot{\varepsilon} > 0)$ represents the (effective) adsorption energy of a competing ion on an adsorbing site. Therefore, φ measures the strength of adsorption of the competing ion. q can be written as

$$q = \beta \exp[(E + kT \ln \tau)/kT] \approx \beta \exp[(x\varepsilon + kT \ln \tau)/kT] \tag{3}$$

where β is virtually a positive constant representing the property of the column, being proportional to the ratio of the effective surface area of the adsorbent to the interstitial volume of the column. $-E\,(E > 0)$ (being approximately equal to $-x\varepsilon$) represents the adsorption energy per sample molecule on adsorbing sites; $-\varepsilon$ represents the adsorption energy per functional adsorption group of the molecule on a site and x the number of functional groups per molecule that are actually used for the adsorption[a]; τ represents the effective number of adsorption configurations which a sample molecule can take on the adsorbent surface (*cf.*, section 5). This means that the term $E + kT \ln \tau$ or $x\varepsilon + kT \ln \tau$ in eqn. 3 represents the absolute value of the adsorption free energy per sample molecule.

---

[a] The protein molecule would fundamentally be represented by a rigid molecular model on the surface of which charged adsorption groups are arranged with slight flexibilities. Actually, however, the protein molecule is adsorbed on either the **a** crystal surface of HA by using negatively charged adsorption groups or the **c** crystal surface by using positively charged adsorption groups; on the **a** and the **c** crystal surface, positively and negatively charged adsorbing sites (C and P sites) are arranged, respectively (see Sections 2–4). It can therefore be deduced that the total energy, $-E$, of a molecule on a crystal surface is contributed to not only the adsorption energy, $-x\varepsilon$, itself but also the repulsive interaction energy between oppositely charged functional groups of the molecule and adsorbing crystal sites. Therefore, to be precise, an expression that is more complicated than that represented in the right-hand side term of eqn. 3 is required. It can be suggested that the abrupt change in the chromatographic behaviour as a function of p*I* (Table 1) can be explained only by taking into account the repulsive interaction effect.

E, x and $\ln \tau$ can be written as

$$E = \sum_{j=1}^{v} \gamma_j E_j \tag{4}$$

$$x \approx \sum_{j=1}^{v} \gamma_j x_j \tag{5}$$

and

$$\ln \tau = -\sum_{j=1}^{v} \gamma_j \ln \gamma_j \tag{6}$$

respectively, where

$$\gamma_j = \frac{\exp(E_j/kT)}{\sum_{j=1}^{v} \exp(E_j/kT)} \qquad \text{(Boltzmann distribution)} \tag{7}$$

In eqns. 4–7, j and v represent the configuration of the molecule on the adsorbent surface and the total number of possible configurations, respectively. $-E_j (E_j > 0)$ and x_j represent the adsorption energy per molecule and the number of functional groups per molecule that are used for the adsorption when the jth-type configuration is being realized, respectively. Eqns. 4–6 show that E, x and $\ln \tau$ represent expectation values of E_j, x_j and $\ln (1/\gamma_j)$ occurring when the Boltzmann distribution (eqn. 7) is realized, respectively.

It can be understood that q (eqn. 3) measures the strength of adsorption of the sample molecule on the adsorbent surface.

Provided that both the sample molecule and the competing ion are adsorbed weakly on adsorbing sites while performing the competition, then the relationship $\varphi m \ll 1$ is fulfilled (see above), and the approximate relationship

$$\varphi m + 1 \approx e^{\varphi m} \tag{8}$$

holds. In this instance, eqn. 2 can be rewritten as

$$\ln k' \approx -x' \varphi m + \ln q \tag{9}$$

indicating that $\ln k'$ decreases linearly with increase in m.

In contrast, provided that both the sample molecule and the competing ion are adsorbed strongly on adsorbing sites, then the relationship $\varphi m \gg 1$ is fulfilled (see above), and the approximate relationship

$$\varphi m + 1 \approx \varphi m \tag{10}$$

holds. In this instance, eqn. 2 can be rewritten as

$$\ln k' \approx -x' \ln m + \ln q - x' \ln \varphi \tag{11}$$

indicating that $\ln k'$ decreases linearly with an increase in $\ln m$.

Concerning study (b), with small sample loads, it is quite general and independent of the adsorption and desorption mechanism that the molarity, m_{elu}, of the gradient element at which the mean part (the centre) of the molecular band is eluted from the column can be represented as a function of the parameter s, defined by [49–51]

$$s = gL \tag{12}$$

where g is the slope of the linear gradient applied, *i.e.*, the increase in molarity per unit length of the column measured from the outlet to the inlet of the column, and L is the total length of the column; s therefore represents the difference in molarity between the inlet and the outlet of the column, which is constant throughout. The function $m_{elu}(s)$ can be implicitly represented [51] by

$$s = \int_{m_{in}}^{m_{elu}} \frac{B(m)}{1 - B(m)} \mathrm{d}m \quad \left[= \int_{m_{in}}^{m_{elu}} \frac{\mathrm{d}m}{k'(m)} \right] \tag{13}$$

where m_{in} is the initial molarity of the gradient.

By substituting eqn. 1 or 2 (competition model) into eqn. 13, the latter can be rewritten as

$$m_{elu}(s) = \frac{1}{\varphi}\{[(x' + 1)\varphi q s + (\varphi m_{in} + 1)^{x'+1}]^{1/(x'+1)} - 1\} \tag{14}$$

In the above, only the chromatographic behaviour at the mean part of the molecular band has been considered. In order to consider the total shape of the band or the chromatographic peak, a theory more fundamental than that presented above is needed [51–53].

Moreover, under overload conditions, account should be taken of mutual interactions among sample molecules occurring in the column, especially on the adsorbent surfaces in the column. Especially with molecules with an asymmetric shape such as those represented by a rod or a prolate spheroid (most of the protein molecules are more or less asymmetric in shape, and a lysozyme molecule, for instance, can approximately be represented by a prolate spheroid of dimensions 45 × 30 × 30 Å [56]), two models were proposed for the phase of the molecules realized on the adsorbent surface [54,55]. Thus, in the first model (called an amorphous phase model), the molecules are situated at random on the adsorbent surface while maintaining a parallel orientation with one another (see below), whereas in the second (called a quasi-crystalline phase model), the positions of the molecules (arranged in parallel with one another) are restricted with respect to one another owing to the repulsive energetic interaction among them through the side of the rod (or the prolate spheroid);

on the basis of a statistical-mechanical consideration, it can, in general, be assumed that the molecules (with a more or less elongated shape) are arranged in parallel with one another on the adsorbent surface while avoiding the mutually superimposed state, provided that the molecular density on the adsorbent surface is high enough [54,55]. Further, by introducing the competition model, it was concluded [54,55] that a rectangular chromatogram is obtained provided that the amorphous phase is realized on the adsorbent surface, whereas a right-angled-triangular chromatogram with tailing is obtained provided that the quasi-crystalline phase is realized (*cf.*, section 7.2). The fact that chromatograms with a shape close to a right-angled triangle with tailing are often experienced under overload conditions implies that the quasi-crystalline phase is realized in many actual instances [54].

7.2. Hydroxyapatite HPLC

HPLC of chicken lysozyme was carried out under different experimental conditions by changing both the total length, L, of the column and the slope of the molarity gradient of the KP buffer; a column packed with HA type S (KB column) was used. A lysozyme molecule (with a basic p*I*) competes with potassium ions from the buffer for adsorption on P sites on the **c** crystal surface of HA (sections 2–4). In accordance with common practice, however, the experimental analysis will be performed below by using the experimental parameters, $m_{\mathrm{elu(P)}}$ and $g'_{\mathrm{(P)}}$ (ϕ = 1 cm) (see Table 1), that are concerned with phosphate ions from the KP buffer; these are two-thirds times as large as the corresponding parameters concerning potassium ions, $m_{\mathrm{elu(K^+)}}$ and $g'_{\mathrm{(K^+)}}$ (ϕ = 1 cm), respectively (see section 1 for the chemical composition of the KP buffer). It should be noted that m_{elu} and m_{in} in eqn. 14 (or eqn. 13) represent $m_{\mathrm{elu(K^+)}}$ and $m_{\mathrm{in(K^+)}}$, or 1.5 $m_{\mathrm{elu(P)}}$ and 1.5 $m_{\mathrm{in(P)}}$, respectively. It should also be noted that g in eqn. 12 (measured in units of M/cm) is concerned with potassium ions from the KP buffer. By measuring the interstitial volume of the column, it can be estimated [30,55] that g [*i.e.*, $g_{\mathrm{(K^+)}}$] is 0.970 times as large as $g'_{\mathrm{(P)}}$ (ϕ = 1 cm) with the KB column. In the analysis, the parameter $s_{\mathrm{app(P)}}$, defined as the product of $g'_{\mathrm{(P)}}$ (ϕ = 1 cm) and L, will also be used instead of s; s is 0.970 times as large as $s_{\mathrm{app(P)}}$.

The points in Fig. 17a are experimental plots of $m_{\mathrm{elu(P)}}$ *versus* L obtained on HA columns for chicken lysozyme for four different $g'_{\mathrm{(P)}}$ (ϕ = 1 cm) values: 5.0, 2.5, 1.25 and 0.45 mM/ml. It can be seen in Fig. 17a that $m_{\mathrm{elu(P)}}$ increases with increases in L and $g'_{\mathrm{(P)}}$ (ϕ = 1 cm) when $g'_{\mathrm{(P)}}$ (ϕ = 1 cm) and L are constant, respectively. The dependence of $m_{\mathrm{elu(P)}}$ on L differs when $g'_{\mathrm{(P)}}$ (ϕ = 1 cm) applied is different, giving four arrangements of the experimental points corresponding to the four values of $g'_{\mathrm{(P)}}$ (ϕ = 1 cm) (see Fig. 17a).

The points in Fig. 17b are plots of $m_{\mathrm{elu(P)}}$ *versus* ln $s_{\mathrm{app(P)}}$ instead of L for the experimental points in Fig. 17a. It can be seen in Fig. 17b that the four arrangements of the experimental points on the [L, $m_{\mathrm{elu(P)}}$] plane (Fig. 17a) converge into a single arrangement when mapped on the [ln $s_{\mathrm{app(P)}}$, $m_{\mathrm{elu(P)}}$] plane. This result is very important as it verifies the correctness of eqn. 13; this should be realized generally, independent of the adsorption and desorption mechanism.

The curve in Fig. 17b is theoretical, calculated by using eqn. 14 in which m_{in} [= $m_{\mathrm{in(K^+)}}$] = 0.0015 M. For the calculation, the optimum value, 25 M^{-1}, of the parameter φ was used [30]. The other parameters, x' and ln q, were evaluated to be 5.7 and 9.5, respectively, in order to have a best fit with the experiment [30]. The lower and

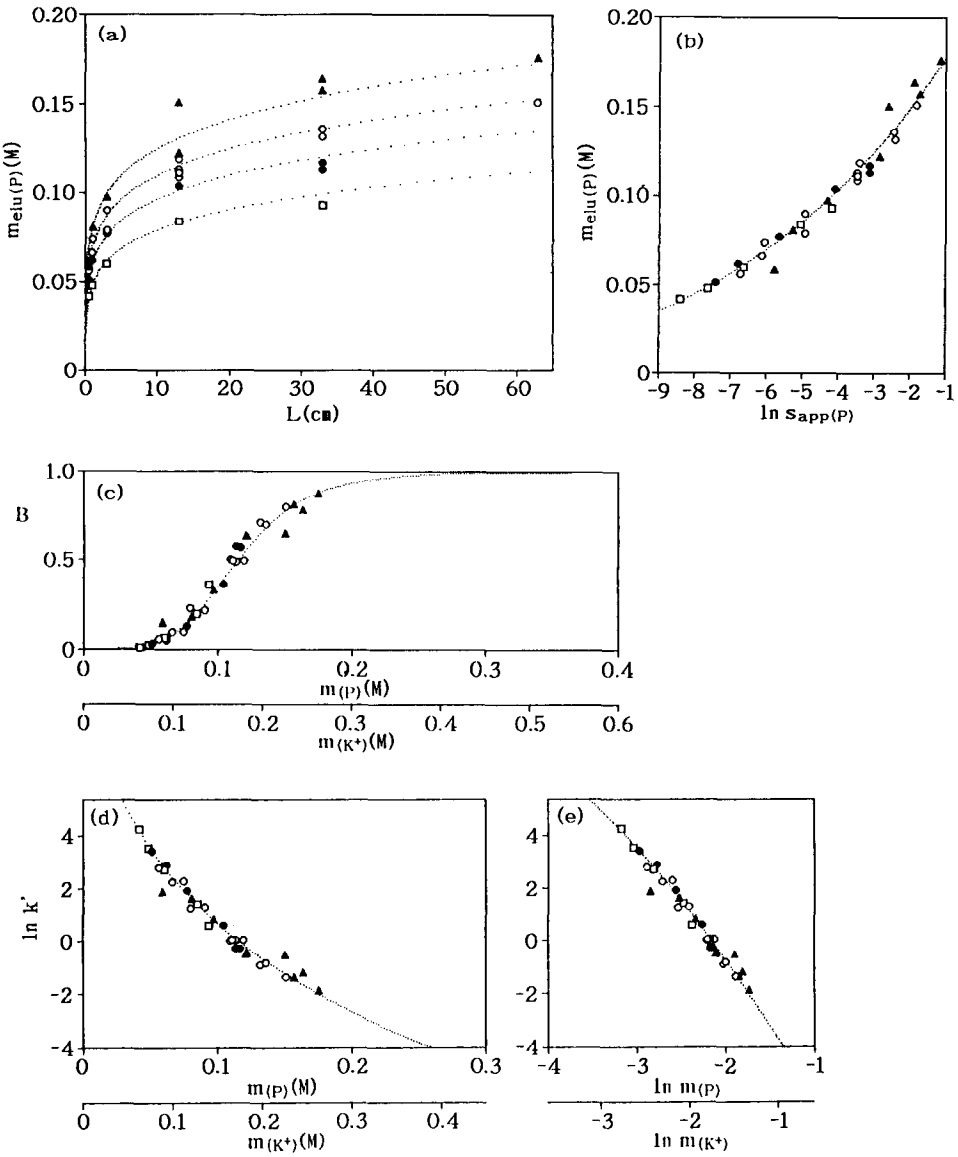

Fig. 17. HPLC analysis of chicken lysozyme, carried out on type S-HA packed KB columns with different lengths; ϕ is always equal to 6 mm. Points in (a)–(e): experimental plots of (a) $m_{elu(P)}$ *versus* L, (b) $m_{elu(P)}$ *versus* ln $s_{app(P)}$, (c) B *versus* $m_{(P)}$ or $m_{(K^+)}$, (d) ln k' *versus* $m_{(P)}$ or $m_{(K^+)}$ and (e) ln k' *versus* ln $m_{(P)}$ or ln $m_{(K^+)}$ for four different $g'_{(P)}$ (ϕ = 1 cm) values: (▲) 5.0, (○) 2.5, (●) 1.25 and (□) 0.45 mM/ml; the corresponding sample loads are 16–30, 20–60, 30 and 50 μg, respectively. Other experimental conditions: $m_{in(P)}$ = 1 mM; flow-rate = 0.5 ml/min; P = 0.3–10.0 MPa; T = 21.0–29.7°C. Curves in (a)–(e): theoretical curves calculated by using (a) eqn. 14, (b) eqn. 14, (c) eqn. 1, (d) eqn. 2 and (e) eqn. 2 (for details, see text). (Reproduced with modifications from ref. 30.)

upper limiting values of x' have been estimated to be 4.0 and 8.0, respectively [30]. It can be seen in Fig. 17b that the coincidence of the theoretical curve with the experimental plot is excellent, explaining a slight displacement from the linearity of the arrangement of the experimental points. This result is also very important as it gives a quantitative verification of the competition model in HA chromatography; the model has qualitatively been deduced from a number of experimental data (section 2). Taking into account both the diameter of the competing potassium ion (section 2) and the arrangement of P sites on the **c** surface (section 4), it is reasonable to assume that a potassium ion covers a single P site when it is adsorbed. Also taking into account the molecular size of lysozyme (45 × 30 × 30 Å; see section 7.1), it can be concluded that the value of 4.0–8.0 for x' that has been estimated above is very reasonable.

Four curves in Fig. 17a were obtained by mapping the theoretical curve in Fig. 17b on the $[L, m_{\mathrm{elu(P)}}]$ plane when $g'_{(P)}$ (ϕ = 1 cm) = 5.0, 2.5, 1.25 and 0.45 mM/ml.

The curve in Fig. 17c is theoretical, representing B for chicken lysozyme as a function of $m_{(P)}$ [or $m_{(K^+)}$]; this was calculated by using eqn. 1. The points in Fig. 17c correspond to the experimental points in Fig. 17a or b mapped on the $\{m_{(P)}$ [or $m_{(K^+)}]$, $B\}$ plane (for the method of mapping, see ref. 30). The curves in Fig. 17d and e are theoretical, representing ln k' for chicken lysozyme as functions of $m_{(P)}$ [or $m_{(K^+)}$] and ln $m_{(P)}$ [or ln $m_{(K^+)}$], respectively; these were calculated by using eqn. 2. The points in Fig. 17d and e represent the experimental points in Fig. 17c (*i.e.*, those in Fig. 17a or b) mapped on the $\{m_{(P)}$ [or $m_{(K^+)}]$, ln $k'\}$ and the $\{$ln $m_{(P)}$ [or ln $m_{(K^+)}]$, ln $k'\}$ plane, respectively. It can be seen in Fig. 17d and e that the arrangement of the experimental points on the $\{m_{(P)}$ [or $m_{(K^+)}]$, ln $k'\}$ and the $\{$ln $m_{(P)}$ [or ln $m_{(K^+)}]$, ln $k'\}$ plane deviate slightly from linearity, being concave and convex, respectively. This indicates that the adsorption of competing ions (and also that of lysozyme) on crystal sites of HA is neither extremely weak nor extremely strong; it is eqn. 2, rather than eqn. 9 or 11, that coincides best with the experiment.

Experimental analyses similar to that performed for lysozyme were applied to other substances [30,57][a], and it was concluded that the x' value, in general, tends to increase slowly with increase in molecular mass [30,57], but that the correlation between molecular mass and x' is weak [30]. The conclusion is consistent with the deduction that the stereochemical structure of the local molecular surface (which is highly characteristic of a molecule, and is intimately related to the x' value) is discerned by the regular crystal surface structure of HA (see section 5).

Fig. 18a, b and c illustrate experimental chromatograms of turkey lysozyme (with a small sample load of 20 μg), turkey lysozyme (with an overload of 15 mg) and a mixture of turkey and chicken lysozymes (with an overload of 15 + 15 mg), respectively; a KB column of I.D. 6 mm and a total length of 13 cm was used, and a linear molarity gradient of the KP buffer with $g'_{(P)}$ = 6.94 mM/ml [$g'_{(P)}$ (ϕ = 1 cm) = 2.5 mM/ml] was applied. Filled and unfilled circles in Fig. 18c represent the contributions of turkey and chicken lysozyme to the total chromatogram as estimated on the basis of the re-chromatography experiment, respectively. It can be seen in Fig. 18 that the position (or the phosphate molarity) at which a chromatogram begins

[a] The experimental analyses for BSA and cytochrome c (in the reduced state) can be seen in Fig. 13. The experimental points and the theoretical curve for lysozyme in Fig. 13b are identical with those shown in Fig. 17b.

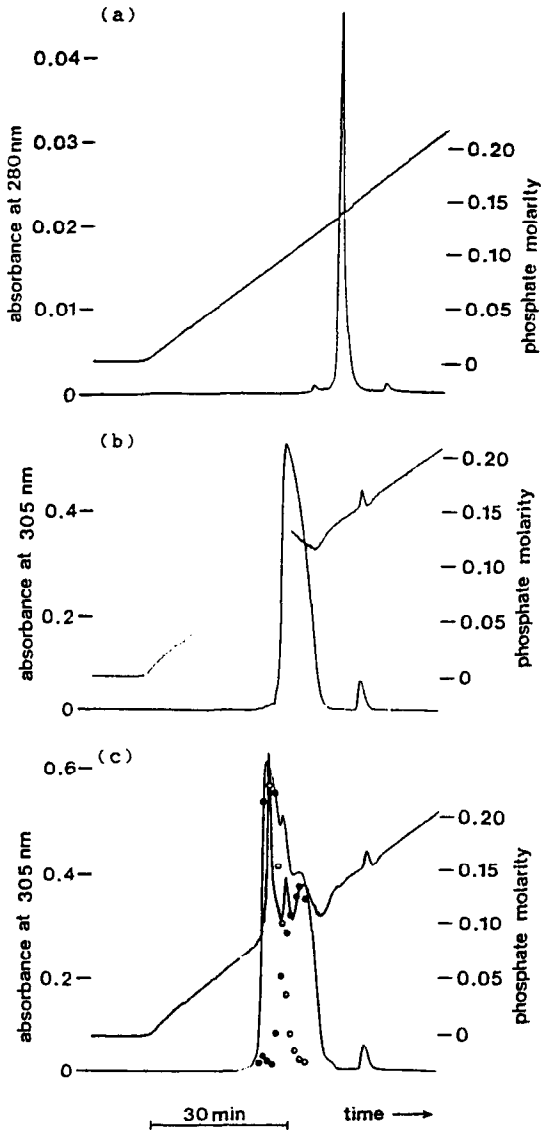

Fig. 18. Experimental chromatograms of (a) turkey lysozyme (20 μg), (b) turkey lysozyme (15 mg) and (c) a mixture of turkey and chicken lysozymes (15 + 15 mg) obtained on a type S-HA packed KB column with ϕ = 6 mm and L = 3 + 10 = 13 cm; a linear molarity gradient of the KP buffer was applied. Experimental conditions: $m_{in(P)}$ = 1 mM; $g'_{(P)}$ = 6.94 mM/ml [$g'_{(P)}$ (ϕ = 1 cm) = 2.5 mM/ml]; flow-rate = 0.5 ml/min; P = 1.8–2.1 MPa; T = 23.5–26.5°C. Filled and unfilled circles in (c) represent the contributions of turkey and chicken lysozymes to the total chromatogram as estimated on the basis of the re-chromatography experiment, respectively. (Reproduced with modifications from ref. 55.)

migrates toward the left (or the low phosphate molarity) as the sample load increases; the width of the chromatogram increases, and the total shape of the chromatogram tends to be close to a right-angled triangle with tailing at the same time. (It can also be

seen in Fig. 18 that, under overload conditions, the gradient is disturbed owing to the presence of the chromatographic peak. This phenomenon is apparent, mainly arising from the disturbance of the refractive index monitoring the gradient [55], *cf.* the legend to Fig. 2.)

Fig. 19a–c illustrate theoretical chromatograms that correspond to the experimental chromatograms in Fig. 18a–c, respectively; these were calculated by using the quasi-crystalline phase model (see section 7.1). (The theoretical chromatogram in Fig. 19a is virtually independent of the model, however, because it represents a chromatogram obtained under a small load condition where the effect of the mutual molecular interaction is negligible.)

The theoretical chromatogram in Fig. 20 corresponds to that shown in Fig. 19b, calculated by using the amorphous phase model (section 7.1). It is evident that it is the

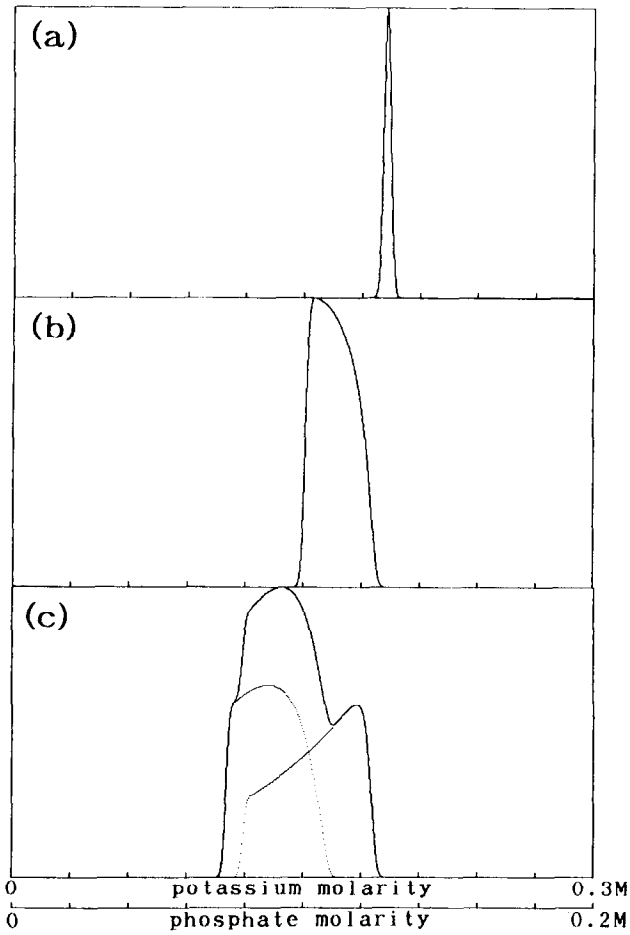

Fig. 19. Parts (a)–(c) represent theoretical chromatograms that correspond to the experimental chromatograms in parts (a)–(c) of Fig. 18, respectively; these were calculated by using the quasi-crystalline phase model. (Reproduced with modifications from ref. 55.)

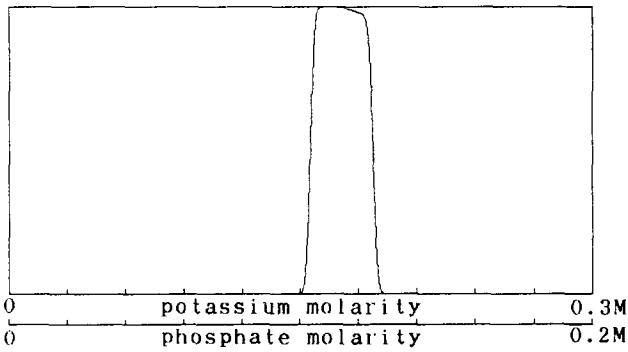

Fig. 20. Theoretical chromatogram corresponding to that in Fig. 19b as calculated by using the amorphous phase model. (Reproduced with modifications from ref. 55.)

quasi-crystalline phase model, and not the amorphous phase model, that gives the best fit with the experiment. The mutual repulsive interaction energy per molecule of lysozyme occurring, provided that the maximum possible contact with other molecules is made on the HA surface, can be estimated to be larger than 0.2–0.4 kcal/mol [55].

REFERENCES

1 A. Tiselius, S. Hjertén and Ö. Levin, *Arch. Biochem. Biophys.*, 65 (1956) 132.
2 G. Bernardi, *Methods Enzymol.*, 21 (1971) 95.
3 G. Bernardi, *Methods Enzymol.*, 22 (1971) 325.
4 G. Bernardi, *Methods Enzymol.*, 27 (1973) 471.
5 B. Moss and E. N. Rosenblum, *J. Biol. Chem.*, 247 (1972) 5194.
6 H. G. Martinson, *Biochemistry*, 12 (1973) 139.
7 H. G. Martinson and E. B. Wagenaar, *Biochemistry*, 13 (1974) 1641.
8 M. Spencer, *J. Chromatogr.*, 166 (1978) 423.
9 M. Spencer, *J. Chromatogr.*, 166 (1978) 435.
10 M. J. Gorbunoff, *Anal. Biochem.*, 136 (1984) 425.
11 M. J. Gorbunoff, *Anal. Biochem.*, 136 (1984) 433.
12 M. J. Gorbunoff and S. N. Timasheff, *Anal. Biochem.*, 136 (1984) 440.
13 T. Kawasaki, S. Takahashi and K. Ikeda, *Eur. J. Biochem.*, 152 (1985) 361.
14 T. Kawasaki, K. Ikeda, S. Takahashi and Y. Kuboki, *Eur. J. Biochem.*, 155 (1986) 249.
15 T. Kawasaki, W. Kobayashi, K. Ikeda, S. Takahashi and H. Monma, *Eur. J. Biochem.*, 157 (1986) 291.
16 T. Kawasaki, M. Niikura, S. Takahashi and W. Kobayashi, *Biochem. Int.*, 13 (1986) 969.
17 T. Kadoya, T. Isobe, M. Ebihara, T. Ogawa, M. Sumita, H. Kuwahara, A. Kobayashi, T. Ishikawa and T. Okuyama, *J. Liq. Chromatogr.*, 9 (1986) 3543.
18 Y. Kato, K. Nakamura and T. Hashimoto, *J. Chromatogr.*, 398 (1987) 340.
19 T. Kawasaki and W. Kobayashi, *Biochem. Int.*, 14 (1987) 55.
20 T. Kawasaki, M. Niikura, S. Takahashi and W. Kobayashi, *Biochem. Int.*, 15 (1987) 1137.
21 T. Sato, T. Okuyama, T. Ogawa and M. Ebihara, *Bunseki Kagaku*, 38 (1989) 34.
22 R. Kasai, H. Yamaguchi and O. Tanaka, *J. Chromatogr.*, 407 (1987) 205.
23 U. Kikkawa, Y. Ono, K. Ogita, T. Fujii, Y. Asaoka, K. Sekiguchi, Y. Kosaka, K. Igarashi and Y. Nishizuka, *FEBS Lett.*, 217 (1987) 227.
24 T. Hatayama, N. Fujio, M. Yukioka, Y. Funae and H. Kinoshita, *J. Chromatogr.*, 481 (1989) 403.
25 Y. Yamakawa, K. Miyasaka, T. Ishikawa, Y. Yamada and T. Okuyama, *J. Chromatogr.*, 506 (1990) 319.
26 Y. Funae and S. Imaoka, *Biochim. Biophys. Acta*, 926 (1987) 349.
27 M. Kikuchi, K. Fukuyama and W. L. Epstein, *Biochim. Biophys. Acta*, 965 (1988) 176.

28 G. Bernardi, M. G. Giro and C. Gaillard, *Biochim. Biophys. Acta*, 278 (1972) 409.
29 G. Bernardi and T. Kawasaki, *Biochim. Biophys. Acta*, 160 (1968) 301.
30 T. Kawasaki, M. Niikura and Y. Kobayashi, *J. Chromatogr.*, 515 (1990) 91.
31 M. I. Kay, R. A. Young and A. S. Posner, *Nature (London)*, 204 (1964) 1050.
32 K. Sudarsanan and R. A. Young, *Acta Crystallogr., Sect. B*, 25 (1969) 1534.
33 J. C. Elliott, P. E. Mackie and R. A. Young, *Science (Washington*, D.C.), 180 (1973) 1055.
34 R. A. Young, *Colloques Internationaux CNRS No. 230: Physico-Chimie et Cristallographie des Apatites d'Intérêt Biologique (Paris)*, CNRS, Paris, 1973, p. 21.
35 T. Kawasaki, *J. Chromatogr.*, 151 (1978) 95.
36 T. Kawasaki, *J. Chromatogr.*, 157 (1978) 7.
37 T. Kawasaki, M. Niikura and Y. Kobayashi, *J. Chromatogr.*, 515 (1990) 125.
38 H. Monma, S. Ueno, M. Tsutsumi and T. Kanazawa, *Yogyo Kagaku Shi*, 86 (1978) 28.
39 W. E. Brown, *Nature (London)*, 196 (1962) 1048.
40 D. R. Taves and R. C. Reedy, *Calcif. Tissue Res.*, 3 (1969) 284.
41 S. M. Krane and M. J. Glimcher, *J. Biol. Chem.*, 237 (1962) 2991.
42 K. Lonsdale, *Nature (London)*, 217 (1968) 56.
43 T. Isobe and T. Okuyama, *Kagaku*, Suppl. 102 (1984) 141.
44 K. Inaka, A. Hasegawa, M. Kubota, K. Takeda, R. Kamijo, K. Konno and M. Ikehara, presented at the *2nd International Conference on Tumor Necrosis Factor and Related Cytokines, Napa, CA*, 1989.
45 T. Kawasaki, *Sep. Sci. Technol.*, 23 (1988) 601.
46 T. Kawasaki, *Sep. Sci. Technol.*, 23 (1988) 617.
47 T. Kawasaki, *Sep. Sci. Technol.*, 23 (1988) 1105.
48 T. Kawasaki, *Biopolymers*, 9 (1970) 277.
49 T. Kawasaki, *J. Chromatogr.*, 93 (1974) 337.
50 T. Kawasaki, *J. Chromatogr.*, 93 (1974) 313.
51 T. Kawasaki, *Sep. Sci. Technol.*, 22 (1987) 121.
52 T. Kawasaki, *Sep. Sci. Technol.*, 23 (1988) 451.
53 T. Kawasaki, *Sep. Sci. Technol.*, 23 (1988) 2365.
54 T. Kawasaki, *Sep. Sci. Technol.*, 24 (1989) 1109.
55 T. Kawasaki and M. Niikura, *Sep. Sci. Technol.*, 25 (1990) 397.
56 T. Imoto, L. N. Johnson, A. C. T. North, D. C. Phillips and J. A. Pulpley, in P. D. Boyer, H. Lardy and K. Myrbäck (Editors), *The Enzymes*, Vol. 7, Academic Press, New York, 1972, p. 692.
57 T. Kawasaki and S. Takahashi, *Sep. Sci. Technol.*, 23 (1988) 193.